UNIVERSITY OF OTTAWA

Chemical and Stable Isotopic Characterization of Geofluids from an Unconventional Natural Gas Field in New Brunswick, Canada

By

David Barton

A THESIS
SUBMITTED TO THE FACULTY OF GRADUATE STUDIES
IN PARTIAL FULFILLMENT OF THE REQUIREMENTS FOR THE
DEGREE OF MASTER OF SCIENCE

DEPARTMENT OF EARTH AND ENVIRONMENTAL SCIENCES
OTTAWA, ONTARIO

March 2018

Abstract

The McCully gas field is located approximately 10 km from the town of Sussex in southern New Brunswick, Canada. There are currently 32 active natural gas production wells which produce dry gas and condensates from the low-permeability Hiram Brook sandstone and Frederick Brook shale members of the Carboniferous Albert formation. The wells range from inclined to vertical, and have been hydraulically fractured in order to stimulate production. This study provides new geochemical data that allows for characterization of deep fluids in the McCully field and the porewaters in four shallow cores from fractured sandstone and siltstone units drilled adjacent to gas wells.

Deep formation fluids of the Hiram Brook and Frederick Brook reservoirs were characterized by sampling production gas and produced water from the wellheads of production wells. Chemical and stable isotope compositions of the gas samples were determined by gas chromatography (GC) and gas-chromatography isotope-ratio-mass-spectroscopy (GC-IRMS), and compositions of the water samples were determined by inductively-coupled-plasma mass spectroscopy (ICP-MS), optical-emission spectroscopy (ICP-OES), and isotope-ratio mass spectroscopy (IRMS). Results indicate that gas compositions differ significantly between the two reservoirs, with the deeper Frederick Brook displaying greater maturity and evidence of isotope reversal. Results from the production water samples indicate that the salinity of formation water is as high as 53,600 mg/kgw (milligrams per kilogram water), and that salinity of the formation water was likely derived from a marine source. However, the strength of conclusions about the formation water composition is limited because the produced water was affected by refluxing in the wellhead, and by the formation of precipitates after sampling.

Porewater from low-permeability drill-core samples was extracted using the 'paper-absorption' method. Vertical composition profiles were prepared for four observation wells, and the data indicate that porewater composition in these rocks is strongly controlled by lithology, redox conditions, and proximity to fractures that act as conduits for meteoric water.

Acknowledgements

I would like to gratefully acknowledge the many people who have helped with this work. First, I would like to thank my supervisor Tom Al for providing invaluable guidance and insight throughout this project. I would also like to thank my co-supervisor Christine Rivard for her guidance and for welcoming me to the GSC. It has been a pleasure working with both of them and I greatly appreciate their unwavering interest in this project.

There are a number of people at the University of Ottawa and the GSC without whom this project would not have been possible. A huge thanks to Paul Middlestead, Patricia Wickham, Wendy Abdi, and Kerry Klassen at the G. G. Hatch Stable Isotope lab for all of their assistance and guidance in exploring the mysterious world of stable isotope geochemistry. Another huge thanks to Nimal DeSilva, Ping Zhang, and Smita Mohanty at the Geochemistry lab for their guidance and support in running the hundreds of samples that I prepared over the past two years. Yet another huge thanks to Xavier Malet and Cindy Bourgault at the GSC for allowing me to join them on a thoroughly entertaining and successful drilling campaign in New Brunswick. And a final huge thanks to everyone else that helped along the way including Geneviève Bordeleau, Denis Lavoie, and the members of Tom's ever-growing research group for their help with everything from obtaining government security clearance, to providing complex scientific advice, and hitting rocks with hammers.

I gratefully acknowledge Natural Resources Canada and the Natural Sciences and Engineering Research Council (Discovery Grant to T. Al) for funding this work, and Corridor Resources for permitting us to work at the McCully Gas Field and for providing us samples, data, information, and support through the duration of this project.

Finally, I would like to thank my friends and family for their support and encouragement over the years. And of course, to everyone taking the time to read this, Thank you, Merci beaucoup, Muito obrigado.

Table of Contents

Abstract ii

Acknowledgements iv

Table of Contents V

List of Tables Vii

List of Figures Viii

Chapter 1 – Introduction 1

1.1 Natural gas, unconventional reservoirs, shale gas, and hydraulic fracturing 1

1.2 Hydrocarbon production in New Brunswick 3

1.3 Objectives 6

1.4 Thesis structure 6

1.5 References cited 7

Chapter 2 – Geochemical characterization of deep fluids in the McCuly Gas Field 9

2.1 Introduction 9

2.2 Study Area 13

2.2.1 Moncton Basin 13

2.2.2 Frederick Brook (FB) Member 14

2.2.3 Hiram Brook (HB) Member 15

2.2.4 The McCully gas field 15

2.3 Sampling and analytical methods 17

2.4 Results and Discussion 20

2.4.1 Gas Composition 20

2.4.2 Produced Water 28

2.5 Conclusions 35

2.6 Conceptual Model 36

2.7 References Cited 37

Chapter 3 – Characterization of porewater in low permeability fractured bedrock aquifers in Southern New Brunswick 43

3.1 Introduction 43

3.2 Study Area and Fieldwork 44
3.3 Materials and Methods 52
3.3.1 Cellulose paper preparation 52
3.3.2 Sampling 52
3.3.3 Core preparation (core cleaving and paper insertion) 53
3.3.4 Leaching 53
3.3.5 Extracted water mass measurement 54
3.3.6 Evaporation 54
3.3.7 Analytical methods and quality control 54
3.3.8 Blanks 55
3.4 Results and Discussion 56
3.4.1 Analytical methods and quality control 56
3.4.2 Contamination bias correction for porewater samples 59
3.4.3 Absorbed porewater mases 59
3.4.4 Uncertainty in porewater concentrations 64
3.4.5 Geologic controls on porewater composition 70
3.5 Conclusions 70
3.5.2 Recommendations for future work 71
3.6 References cited 73

List of Tables

Table 2.1:	Composition of gases from the McCully gas field	21
Table 2.2:	Major ion and stable isotope composition of McCully production water samples	30
Table 3.1:	Summary of McCully and Elgin porewater extractions	45
Table 3.2:	Solute concentrations of blanks samples in comparison with porewater leachate samples	58
Table 3.3:	Results of porewater extraction and characterization	60
Table 3.4	Relative standard deviation of porewater concentrations	65

List of Figures

Figure 1.1	Plot of natural gas production in the United States between 2000 and 2015 by source	2
Figure 1.2	Plot of natural gas consumption in the United States between 2000 and 2016	3
Figure 1.3	Map of New Brunswick showing locations of the McCully gas field and Maritimes & Northeastern pipeline	4
Figure 1.4	Plot of natural gas production in New Brunswick compared to Canada as a whole between 1947 and 2015	5
Figure 2.1:	Map of New Brunswick showing location of McCully Gas Field	12
Figure 2.2:	Stratigraphy of the Maritimes Basin	13
Figure 2.3:	Geologic cross section of the Moncton basin showing geology of the McCully gas field	16
Figure 2.4:	Map showing locations of sampled wells in the McCully gas field	19
Figure 2.5:	Bernard plot of McCully gas samples	22
Figure 2.6:	Schoell plot of McCully gas samples	22
Figure 2.7:	Natural gas plots of McCully gas samples	23
Figure 2.8:	Plot of $\delta^{13}C_{methane}$ Vs $\delta^{13}C_{ethane}$ of McCully gas samples	24
Figure 2.9:	Plot of C_{4+} concentrations (%volume) Vs ($\delta^{13}C_{methane}$ - $\delta^{13}C_{ethane}$) of the McCully gas samples	24
Figure 2.10:	Plot of $\delta^{13}C_{methane}$ - $\delta^{13}C_{ethane}$ (‰ VPDP) Vs iso-butane/n-butane of the McCully gas samples	25
Figure 2.11:	Chloride normalized cross-plots of major ions from McCully production water samples	31
Figure 2.12:	Cross plot of $\delta^{18}O$ and $\delta^{2}H$ of McCully produced water samples	32
Figure 2.13:	Cross plot of $\delta^{18}O$ and total dissolved solids of McCully produced water samples	33
Figure 3.1:	Map of GSC observation wells in McCully and Elgin areas of New Brunswick	45
Figure 3.2:	Selected core samples from PO-07	48
Figure 3.3:	Selected core samples from PO-08	49
Figure 3.4:	Selected core samples from PO-09	50

Figure 3.5: Selected core samples from PO-10 51
Figure 3.6: Vertical geochemical profiles of porewater from PO-07 66
Figure 3.7: Vertical geochemical profiles of porewater from PO-08 67
Figure 3.8: Vertical geochemical profiles of porewater from PO-09 68
Figure 3.9: Vertical geochemical profiles of porewater from PO-10 69

Chapter 1 – Introduction

1.1 Natural Gas, Unconventional Reservoirs, Shale Gas, and Hydraulic Fracturing

Natural gas is a mixture of simple hydrocarbons composed primarily of methane (CH_4) with small quantities of other hydrocarbons such as ethane (C_2H_6), propane (C_3H_8), butane (C_4H_{10}), and non-hydrocarbon components such as nitrogen and carbon dioxide (NRCan, 2015; EIA, 2016a). Natural gas is formed by the decomposition of the complex organic molecules which make up deceased plants and animals. This process may take place in environments such as landfills, marshes, and shallow geologic settings, in which case it is driven by bacteria, and is described as *biogenic* gas. Biogenic natural gas is composed almost entirely of methane which, due to the effects of kinetic isotope fractionation, is depleted in the heavier isotopes of carbon and hydrogen. Natural gas generated in deep geologic environments, where the process is driven by intense heat and pressure, is referred to as *thermogenic* gas. Thermogenic natural gas contains larger concentrations of C_{2+} hydrocarbons, and is enriched in the heavier isotopes of carbon and hydrogen compared to biogenic gas. The majority of commercially exploited natural gas is thermogenic in origin, and is either produced from so-called *conventional* geologic reservoirs, consisting of a permeable *reservoir* rock such as sandstone, confined by a lower-permeability *caprock* unit; or from so-called *unconventional* reservoirs, consisting of or a low-permeability rocks such as shale which may act as both a source and reservoir for hydrocarbons. Due to the low permeability of the reservoir rock in the case of unconventional reservoirs, gas migration is extremely slow, and a stimulation technique such as hydraulic fracturing is required to allow for gas to be produced economically. When a reservoir is hydraulically fractured, a fluid such as

water, along with small concentrations of chemical additives and a proppant such as sand, is injected at high pressure. Injection of the fluid creates fractures within the reservoir, while the proppant acts to hold the fractures open. Hydraulic fracturing has been so effective in accessing untapped resources that hydraulically fractured shale reservoirs are now the largest source of natural gas produced in the United States (Fig. 1.1). The surge in production from shale reservoirs has had major implications in the United States, where consumption of natural gas for electricity generation has roughly doubled since 2000, making it the largest source for electric power generation (Fig. 1.2) (EIA, 2017b). The effects of unconventional gas development are also evident in Canada, not in the hydropower dominated electricity generation sector, but in exports to the United States, which account approximately 51% of all Canadian production (NRCan, 2017a).

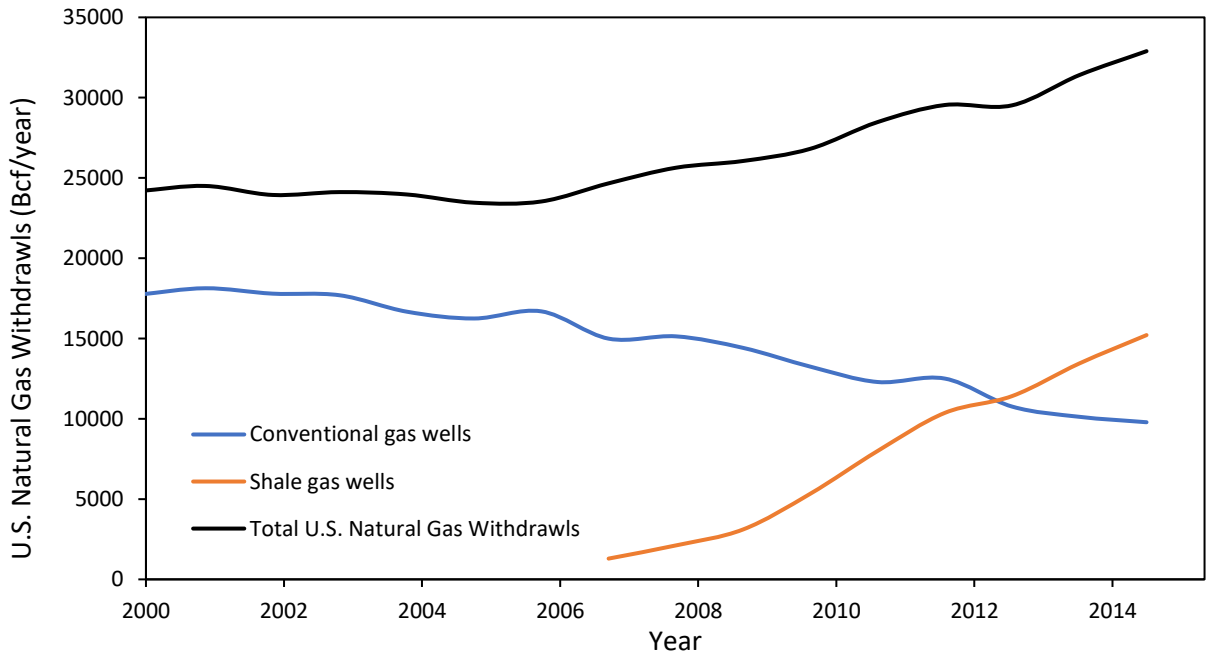

Figure 1.1. Natural gas production in the United States between 2000 and 2015. Production from conventional wells (EIA, 2017c), shale gas wells (EIA, 2017d), total withdrawals (EIA, 2017e). Production of natural gas from oil wells is not included.

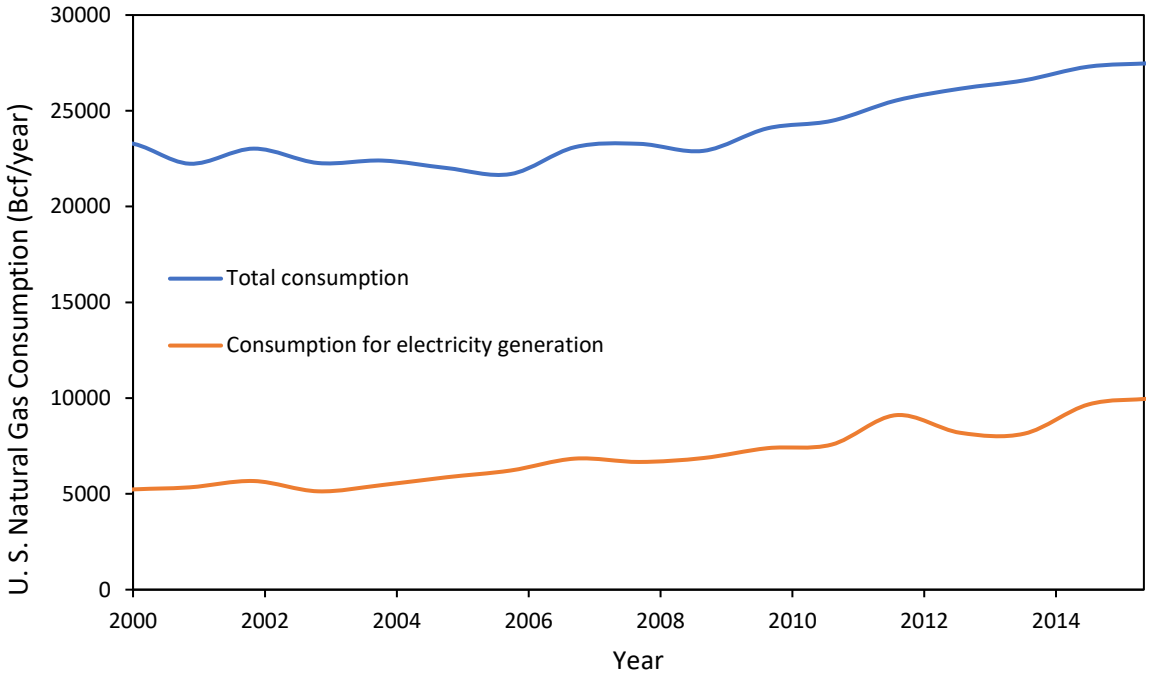

Figure 1.2. Natural gas consumption in the United States between 2000 and 2016. Consumption for electricity generation (EIA, 2017f), total consumption (EIA, 2017g).

1.2 Hydrocarbon Production in New Brunswick

New Brunswick has a long history of commercial hydrocarbon production, dating back to the 1850's when oil-shale and albertite deposits were mined from the lower Carboniferous Albert Formation (Park, 2014). In 1859, the first hydrocarbon well in Canada was drilled near Moncton, and was followed by several decades of sporadic exploration and development with limited success (St. Peter, 2000). In 1909 the Stoney Creek oil field, the most successful hydrocarbon development in New Brunswick's history, was discovered roughly 15km south of Moncton (St. Peter, 2000). The Stoney Creek field produces oil and natural gas from the Albert Formation, and has been in nearly continuous operation since its discovery, with a break in production between 1991 and 2007 (St. Peter, 2000). In 2000, natural gas was discovered in a tight sandstone reservoir

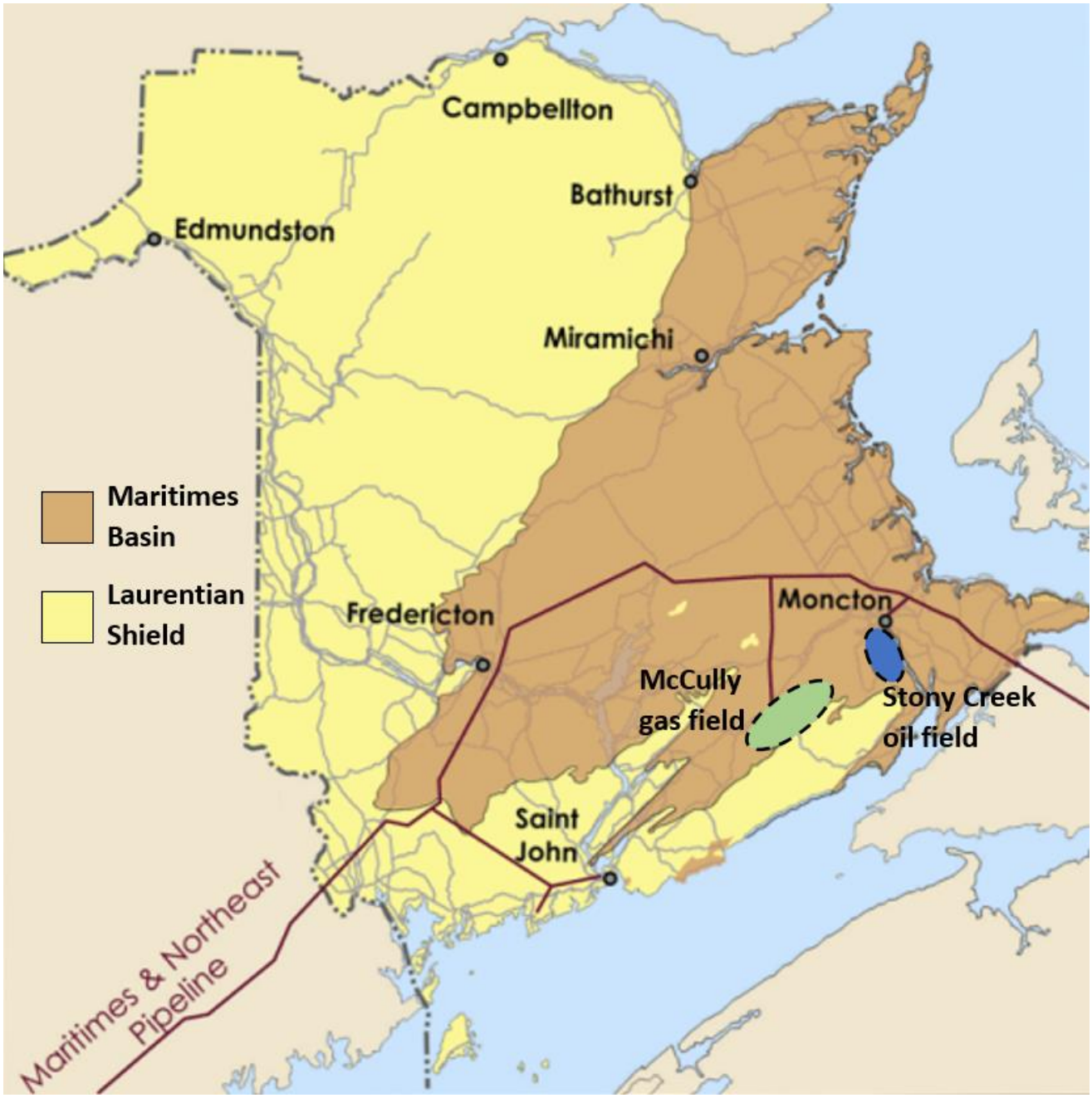

Figure 1.3. Map of New Brunswick showing McCully gas field and Maritimes & Northeastern pipelines. Modified from Government of New Brunswick, 2017.

at what is now the McCully gas field outside of the town of Sussex in southern New Brunswick. The first discovery wells in the McCully field were intended for the disposal of brine from a nearby potash mine (NRCan, 2017b). Since its discovery, 39 vertical and inclined wells have been drilled and hydraulically fractured in the Hiram Brook (tight sandstone) and underlying Frederick Brook

(shale) members of the Albert Formation. Production from the McCully field has been tied in to the Maritimes and Northeastern pipeline, connecting it to the northeastern U.S. market (Fig. 1.3) (Corridor Resources, 2017). Development of the McCully field has led to a substantial increase in natural gas production in New Brunswick, although the province remains a relatively small player within the industry. In 2008, Natural gas production in New Brunswick reached an all-time high of 258 billion cubic meters, representing approximately 0.13% of total Canadian production (Fig. 1.4) (CAPP, 2017). In 2014, the government of New Brunswick issued a moratorium on the use of hydraulic fracturing in response to public concerns regarding environmental issues, including potential adverse effects on groundwater resources (NRCan, 2017b). Exploration for unconventional gas resources in New Brunswick has since stopped, although production from existing wells continues.

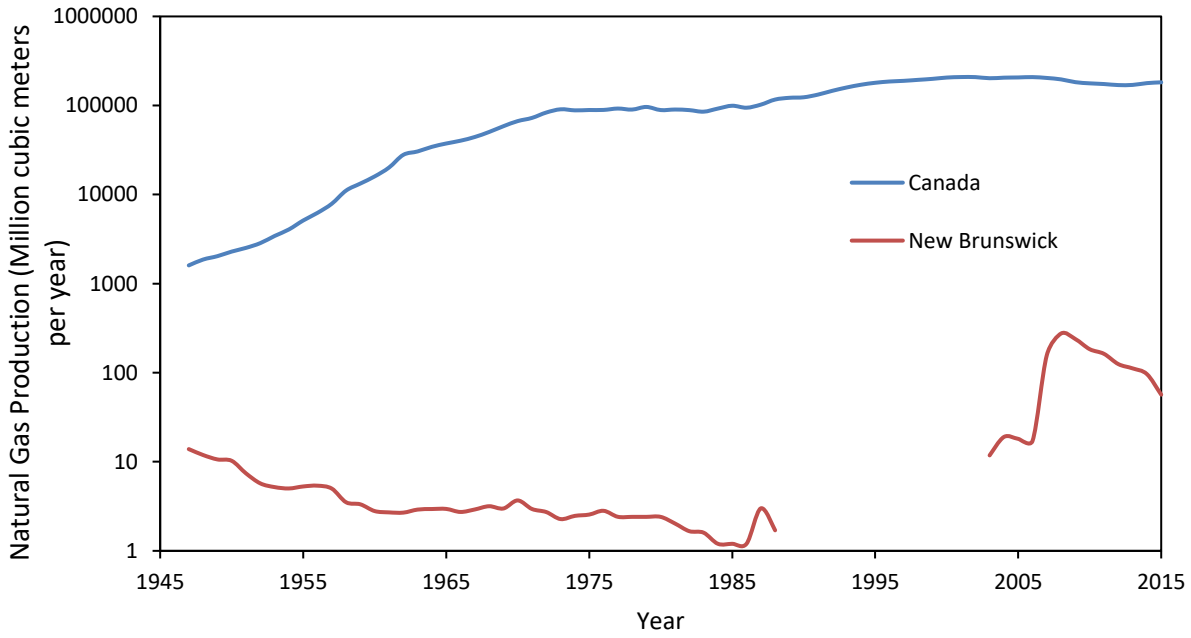

Figure 1.4. Natural gas production in New Brunswick compared to total Canadian production between 1947 and 2015, from CAPP (2017)

1.3 Objectives

The primary objective of this thesis is to characterize the chemical and stable-isotope compositions of deep fluids from the McCully gas field, and shallow groundwater in the vicinity of the field, in order to better understand their composition and provenance. This thesis is intended to add to the body of published scientific literature pertaining to the McCully gas field, and to aid in policy development regarding the future of hydrocarbon development in the province of New Brunswick.

1.4 Thesis Structure

This thesis is organized in article format, where the body of the thesis consists of two independent chapters with the intention that the first chapter (Chapter 2) will be submitted to a scientific journal for publication.

Chapter 2 consists of a geochemical characterization of produced fluids from the McCully gas field. This study was undertaken as part of a larger project led by Dr. Christine Rivard at the Geological Survey of Canada Québec division, with the objective of assessing groundwater vulnerability from shale-gas activities in the Sussex area of southern New Brunswick. The objective of this specific study was to characterize the deep end-member compositions of fluids within the gas field.

Chapter 3 describes an experiment undertaken to characterize the porewaters in core samples from four shallow observation wells drilled in fractured sandstone and siltstone units on well pads adjacent to gas wells at the McCully gas field. This experiment was intended to

complement the larger project by producing high-resolution geochemical profiles of porewater composition within the fractured bedrock under consideration.

1.5 References Cited

Canadian association of petroleum producers. (2017). *Statistical handbook for Canada's upstream petroleum industry.* Retrieved from http://www.capp.ca/publications-and-statistics/statistics/statistical-handbook

Corridor Resources. (2017). *Corporate presentation.* Retrieved from https://www.corridor.ca/your-investment/events-presentations/

EIA. (2016a). *Natural gas explained*. Retrieved from https://www.eia.gov/energyexplained/index.cfm?page=natural_gas_home

EIA. (2017b). *Electricity in the United States*. Retrieved from https://www.eia.gov/energyexplained/index.cfm?page=electricity_in_the_united_states

EIA. (2017c). *U.S. Natural gas gross withdrawals from gas wells.* Retrieved from https://www.eia.gov/dnav/ng/hist/n9011us2m.htm

EIA. (2017d). *U.S. Natural gas gross withdrawals from shale gas.* Retrieved from https://www.eia.gov/dnav/ng/hist/ngm_epg0_fgs_nus_mmcfm.htm

EIA. (2017e). *U.S. Natural gas gross withdrawals.* Retrieved from https://www.eia.gov/dnav/ng/hist/n9010us2m.htm

EIA. (2017f). *U.S. Natural gas total consumption.* Retrieved from https://www.eia.gov/dnav/ng/hist/n9140us2A.htm

EIA. (2017g). *U.S. Natural gas deliveries to electric power consumers.* Retrieved from https://www.eia.gov/dnav/ng/hist/n3045us2A.htm

Government of New Brunswick. (2017). *New Brunswick oil and gas.* Retrieved from http://www2.gnb.ca/content/dam/gnb/Corporate/pdf/ShaleGas/en/History.pdf

NRCan. (2015). *Natural gas: a primer.* Retrieved from http://www.nrcan.gc.ca/energy/natural-gas/5641

NRCan, (2017). *Energy fact book 2016-2017.* Retrieved from https://www.nrcan.gc.ca/sites/www.nrcan.gc.ca/files/energy/pdf/EnergyFactBook_2016_17_En.pdf

NRCan. (2017b). *New Brunswick's shale and tight resources.* Retrieved from http://www.nrcan.gc.ca/energy/sources/shale-tight-resources/17698

Park, F. A. (2014). Shale gas in New Brunswick: geological background. In Saillant, R & Campbell, D (Eds.), *Shale gas in New Brunswick towards a better understanding.* Moncton, NB: Canadian institute for research on public policy and public administration.

St. Peter, C. (2000). *Oil and natural gas in New Brunswick: historical and current industry-related activities.* Retrieved from http://www2.gnb.ca/content/dam/gnb/Departments/en/pdf/Minerals-Minerales/ONG_History-E.pdf

Chapter 2 - Chemical and Isotopic Characterization of Formation Fluids from an Unconventional Gas Field in New Brunswick, Canada

2.1 Introduction

Production of natural gas from unconventional reservoirs such as shales and tight sandstones, has increased dramatically in the United States and Canada over the past decade. The increase can be attributed to advancements in the practice of hydraulic fracturing in horizontal wells, a process wherein a fluid, typically water, along with chemical additives and a proppant such as sand or ceramic beads, is injected at high pressure into a target geologic unit (EPA, 2017; NRCan, 2016a). Injection of the fluid generates a fracture network in the reservoir rock, through which hydrocarbons trapped in the tight pore system are able to migrate to the production well. Natural gas produced from hydraulically fractured, unconventional reservoirs now accounts for more than half of all production in the United States and approximately half of all production in Canada (Perrin and Cook, 2016; NRCan, 2016b).

In addition to unlocking major new supplies of natural gas, exploration and production from unconventional reservoirs is shedding light on the geochemistry of previously unexplored regions of the subsurface, leading to new insight into the processes of thermogenic natural gas generation. Among these, is the prevalence of isotopically "reversed" natural gas, in which the $\delta^{13}C$ value of the methane fraction is enriched relative to that of ethane, which is in turn enriched relative to propane (Tilley and Muehlenbachs, 2013). Isotopically reversed gases defy the "normal" isotopic trend of progressive ^{13}C depletion with decreasing carbon number that results from kinetic isotope fractionation during kerogen cracking that is observed in conventional

reservoirs as well as gas produced in most laboratory pyrolysis experiments (Chung et al. 1988; Golding et al. 2013, Gao et al. 2014). Isotopically reversed natural gas has been observed in numerous unconventional reservoirs throughout the United States, Canada, and China, and is of particular interest as its occurrence is often associated with high productivity and low rates of decline (Ferworn et al. 2008; Burruss and Laughrey, 2010; Tilley et al. 2011; Zumberge et al, 2012; Zeng et al. 2011; Chatellier et al, 2013; Dai et al. 2017; Zhang et al. 2017). Several conceptual models have been proposed to explain isotopic reversals, including secondary cracking of liquid hydrocarbons, redox reactions involving transition metals, and water-hydrocarbon reactions, though it is possible that there are multiple contributing factors (Golding et al. 2013; Tilley and Muehlenbachs, 2013). While there is still uncertainty in the specific causes and mechanisms, the high-pressure, closed system conditions typical of shale and tight sandstone reservoirs, and the presence of water, appear to be common factors in systems that display isotopic reversal.

In eastern Canada, the Utica and Frederick Brook shales located in Quebec and New Brunswick, respectively, are regarded as potentially significant sources of natural gas and have been the targets of exploration and preliminary development. However, exploration has been stopped in both provinces since the imposition of an official moratorium on hydraulic fracturing in New Brunswick in 2014, and a *de-facto* moratorium in the St. Lawrence Lowlands of Quebec in 2010. There is a long history of commercial hydrocarbon production in New Brunswick, dating back to the 1850`s when the province was an exporter of bitumen mined from oil-shale and albertite deposits within the Albert Formation (Park, 2014). The first hydrocarbon well in Canada was drilled in New Brunswick in 1859 near Moncton (St. Peter, 2000). The Most successful development in New Brunswick is the Stony Creek oil field (Fig. 2.1) which was discovered in 1909

and has produced oil and natural gas from the Albert Formation almost continuously since then. As of 2017, it is estimated that there are technically recoverable natural gas reserves of up to 78 trillion cubic feet in New Brunswick (NRCan, 2017a), representing approximately 4.4 to 9% of total technically recoverable natural gas reserves in Canada (NRCan, 2017b). Despite this large potential, there are currently only 32 producing gas wells in the province, all of which produce from the tight sandstone and shale reservoirs of the McCully gas field (Fig. 2.1; Corridor Resources, 2017). The objective of this study was to provide a thorough geochemical characterization of the deep formation fluids in the McCully gas field in order to better understand their origins. This study was part of a larger project focusing on shallow aquifer vulnerability to shale gas activities (Rivard et al. 2017), and builds upon work by Al et al. (2013).

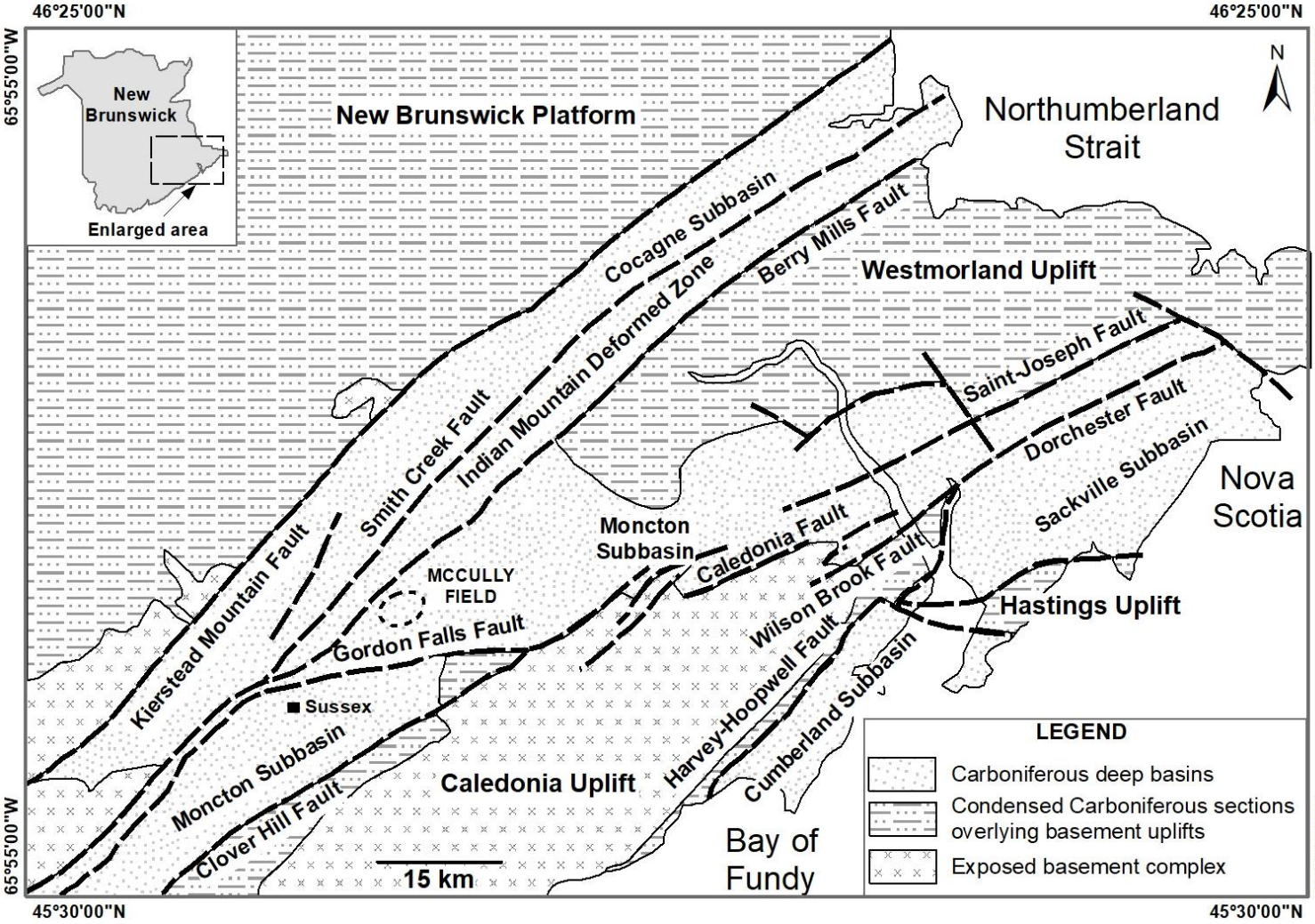

Figure 2.1. Location of the McCully gas field. Modified from Government of New Brunswick, 2018a.

2.2 Study Area

2.2.1 Moncton Basin

Stratigraphy of the Moncton Basin, also referred to as the Moncton *sub*-basin, is late Devonian to Pennsylvanian in age, and consists mostly of rocks of fluvio-lacustrine origin with the exception of the Windsor Group, which is a Viséan aged succession of marine carbonates and evaporites (Fig. 2.2) (Wilson and White, 2006). The basal unit of the Moncton basin is the Horton Group, within which the Memramcook Formation, a series of red-grey conglomerates, overlies the igneous and metamorphic basement complex. Conformably overlying the Memramcook Formation is the Albert Formation, a fluvio-lacustrine sequence composed mostly of shales and sandstones, including the kerogenous shales and tight sandstones of the Frederick Brook (FB) and Hiram Brook (HB) members respectively. The maximum burial depth of the Albert Formation has been estimated at roughly five kilometers, between two and three kilometers greater than its present maximum depth, indicating that significant uplift and erosion has taken place (St Peter, 1992; Chowdhury and Noble, 1996). The Horton Group is unconformably overlain by the Sussex Group, which consists mostly of lacustrine red-beds. The Windsor Group is the only

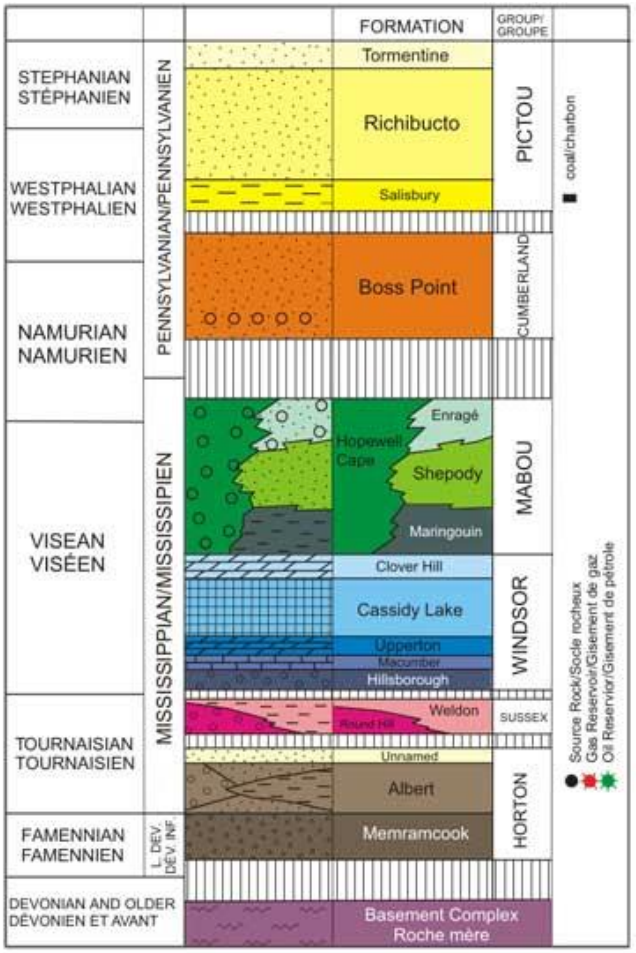

Figure 2.2. Stratigraphy of the Maritimes Basin (Government of New Brunswick, 2018b)

definitively marine succession of the basin, it unconformably overlies the Sussex Group. The Windsor Group is a third order transgressive-regressive depositional sequence in which the basal carbonate units represent the transgressive system. These units are overlain by thick evaporite, and subordinate clastic units, which form a high-stand to forced regressive system tract which caps the sequence. Anhydrite, halite, and various potash minerals were mined from the Windsor Group at various locations in Southern New Brunswick between 1983 and 2016. Finally, the Mabou Group overlies the Windsor Group, and is now exposed at ground surface in the Sussex area. The Mabou Group consists mostly of red-grey mudstones, sandstones, and conglomerates.

2.2.2 Frederick Brook (FB) Member

The FB Member is a kerogenous shale within the Albert Formation that lies between the Dawson Settlement Member below, and the HB member above (Fig. 2.2). Previous studies have described the depositional setting of the FB as a deep, low energy, anoxic, lacustrine environment situated at sub-tropical latitude (Smith and Gibling, 1987; Keighley, 2011). This model is supported by the presence of freshwater fish fossils and abundant type I kerogen which is typical of lacustrine environments (Keighley, 2008). Type II kerogen, which is generally associated with marine environments, as well as marine fossils have been reported in certain areas of the Horton Group, indicating the possibility of limited marine influence (Gussow, 1953; Tissot and Welte, 1984; Smith and Gibling, 1987; Choudry et al. 1991). The FB member is principally composed of illite with abundant pyrite, and is cemented with calcite, dolomite, and ankerite; it is divided into an upper, more siliceous shale, and a lower, more dolomitic shale (Smith and Gibling; 1987, Choudry et al, 1991; Smith et al. 1991; Keighley et al. 2008; Séjourné, 2017).

2.2.3 Hiram Brook (HB) Member

The HB member is dominated by silty sandstone with minor to locally significant shale intervals. The sandstone contains natural gas with some condensates which are believed to have been generated in the shale intervals and possibly the underlying FB shale. The HB is informally divided into seven separate sand units designated A through G (deepest to shallowest). These units are believed to have been deposited during a relative water level regression period following the deposition of the lacustrine FB member, which allowed for progradation of nearshore sands. The HB marks the end of the fluvio-lacustrine succession of the Albert Formation (Keighley et al. 2008). Petrographic studies indicate that the HB member is a grey, very-fine silty sandstone with a porosity of approximately 8%, containing abundant calcite, dolomite, ankerite, and pyrite along with laminated kerogenous shale layers (Keighley and St. Peter, 2015; Chowdhury et al. 1991; Chowdhury and Noble, 1996; Keighley et al. 2008).

2.2.4 The McCully gas field

The McCully gas field is located approximately 10 km from the town of Sussex in southern New Brunswick, Canada. The field covers an area of approximately 114 km^2 and is located over a large anticlinal structure which acts as a trap for hydrocarbons (Keighley and St. Peter 2015). It is situated within the roughly 3700 km^2 Moncton Basin, which is part of the larger Maritimes Basin (Fig. 2.1) (Keighley, 2011; Séjourné, 2017). Natural gas was first discovered at the McCully field in 2000 in a discovery well drilled near a potash mine owned by the Potash Corporation of Saskatchewan Inc. (PCS) (Martel and Durling, 2001; Corridor Resources, 2017). Since the discovery, 39 vertical and inclined wells have been drilled, of which, 26 were drilled in to the HB member and 13 penetrate into the underlying FB member (Fig 2.3) (Corridor Resources, 2017).

Production wells in the McCully field contain multiple perforations across intervals of several hundred meters between depths of approximately 1800 m to 3600 m. As of August 2017, there are 32 active production wells in the McCully field producing dry natural gas and some natural gas condensates (wet gas). All of the wells in the McCully field have been hydraulically fractured to improve production using water-based or liquified petroleum gas (LPG) fluids (Leblanc et al. 2011; Rivard et al. 2014). Cumulative production at the McCully field to the end of 2016 is 54.4 billion cubic feet of dry natural gas (Corridor Resources, 2017).

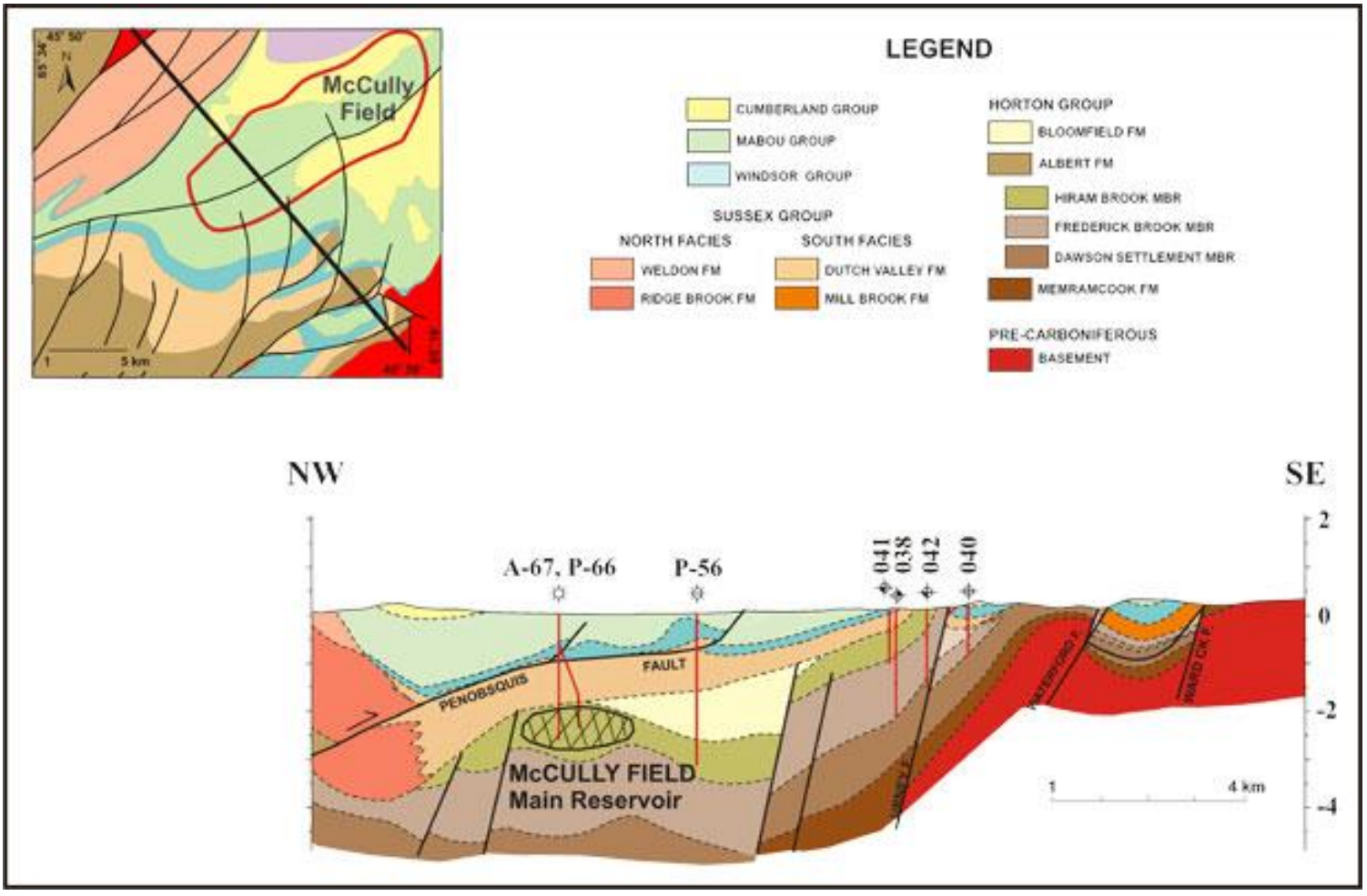

Figure 2.3. Geologic cross section of the Moncton Basin showing the geology of the McCully gas field and the hydrocarbon trap formation of the HB sandstone (Government of New Brunswick, 2018c)

2.3 Sampling and analytical methods

Gas samples were collected from the wellheads of thirteen production wells in the McCully field using a pressure reducing manifold and IsoTube® sample containers (IsoTech Laboratories, Champaign IL, USA). Nine of the production wells that were sampled are drilled into the HB sandstone and four penetrate into the underlying FB shale (Fig. 2.4). All gas analyses were performed at the G.G. Hatch Stable Isotope Laboratory at the University of Ottawa. The chemical composition of the gas samples was measured using an SRI 8610C dual column gas chromatograph fitted with flame ionization and thermal conductivity detectors. Stable carbon, hydrogen, and nitrogen isotope measurements of the hydrocarbon (C_1-C_6), CO_2, and N_2 fractions of the gas samples were performed using a Thermo-Fisher Delta V Isotope Ratio Mass Spectrometer interfaced via a Conflow 4 to an Agilent 8790A gas chromatograph equipped with a combustion furnace for carbon, and a pyrolysis furnace for hydrogen. The $\delta^{13}C$ and $\delta^{2}H$ measurements of pentane and hexane were attempted for all samples, but were only successful for samples with sufficiently high concentration, all of which were produced from the HB.

Produced water samples were collected from the wellheads of nine wells. The samples were collected by Corridor Resources personnel in 1L Nalgene bottles using a time-integrated sampling system. The samples were not acidified or filtered in the field, and it was not possible to measure field parameters (E_h, pH, alkalinity, temperature) representative of subsurface conditions. When the samples were received at the University of Ottawa, black and reddish-brown precipitates as well as separate organic liquid phases were observed in the bottles. A

qualitative examination of the precipitates using Scanning Electron Microscopy and Energy-dispersive X-ray Spectroscopy (SEM-EDS) was performed to assess their composition.

The production water samples were allowed to settle and separate into organic, aqueous, and precipitate phases, at which time aliquots of the aqueous fractions were collected and filtered through 1 μm glass prefilters followed by 0.45 μm nylon filter cartridges using 60 mL plastic syringes. Alkalinity of the filtered production water samples was measured colorimetrically using a Hach digital titrator (Hach Company, Loveland CO). Aliquots (0.5 mL) of production water were treated with activated charcoal, metallic copper chips, and Hokko beads prior to stable isotope analysis ($\delta^{2}H$, $\delta^{18}O$) in the G.G. Hatch Stable Isotope Lab using a Thermo-Fisher Delta Plus XP isotope ratio mass spectrometer, interfaced with a Thermo-Fisher Gasbench II. Filtered water samples were prepared in 1% ultrapure nitric acid solution for analysis of cation (Na, Mg, Ca, K) and total S concentrations by ICP-OES (Varian Vista Pro), and in 1% ultrapure ammonia solution for analysis of Cl and Br concentrations by ICP-MS (Agilent 8800), at the University of Ottawa Geochemistry Lab. Strontium isotope ratios ($^{87}Sr/^{86}Sr$) of filtered water samples were measured using a ThermoFinnigan Triton TI thermal ionization mass spectrometer (TIMS) at the Isotope Geochemistry and Geochronology Research Center at Carleton University in Ottawa Ontario.

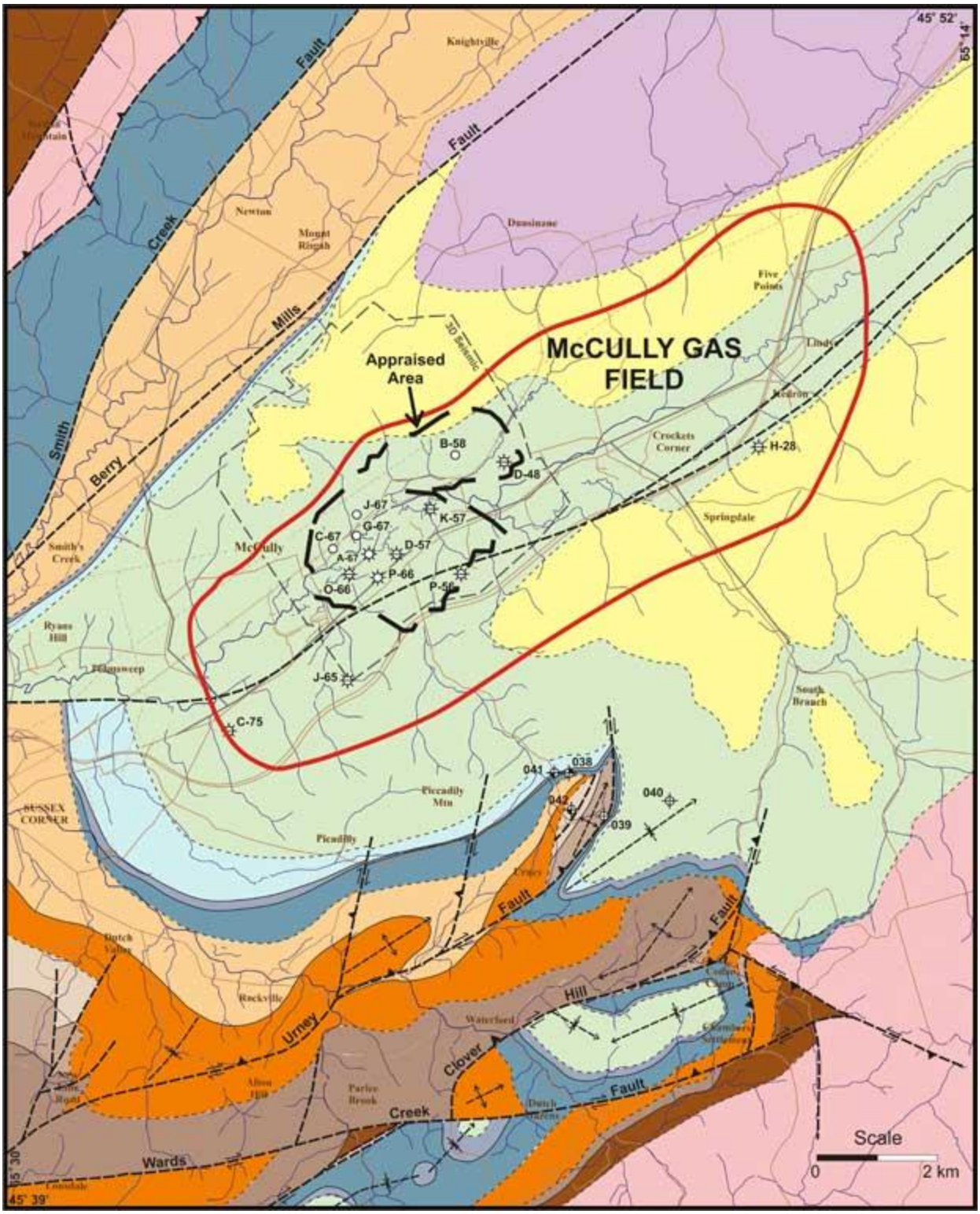

Figure 2.4. Location of natural gas wells in the McCully gas field (Government of New Brunswick, 2018d)

2.4 Results and discussion

2.4.1 Gas Composition

Gas from the McCully field is 95-99% hydrocarbons by volume and is dominated by methane (Table 2.1). Non-hydrocarbon components (N_2, CO_2) occur at concentrations between 0.01-0.09 and 0.47-4.95 vol % respectively, with samples from the FB shale showing the highest concentrations (Table 2.1). Dryness of the gases [$\%C_1/(\Sigma(\%C_1\text{-}C_6)$] ranges from 90-98% with no evident trend toward increasing dryness with production depth. Stable isotope compositions of the gases (Table 2.1) are variable and show a trend of ^{13}C enrichment in the methane fraction of the FB gases relative to the HB samples (Figs. 2.5 and 2.6). All but one of the samples produced from the HB reservoir follow the "normal" isotopic profile ($\delta^{13}C_1<\delta^{13}C_2<\delta^{13}C_3<\delta^{13}C_4$) while all of the samples from the FB shale are partially reversed ($\delta^{13}C_1>\delta^{13}C_2<\delta^{13}C_3<\delta^{13}C_4$) or fully reversed ($\delta^{13}C_1>\delta^{13}C_2\geq\delta^{13}C_3>\delta^{13}C_4$), with $\delta^{13}C_2$ equal to $\delta^{13}C_3$ within the margin of analytical uncertainty of 0.3‰ (Figs. 2.7A,B, 2.8). The majority of samples from the McCully field do not display linear relationships between $\delta^{13}C$ and carbon number, as is predicted in kinetic isotope fractionation models (Chung et al. 1988). Rather, most samples display a kinked, or V-shaped profile, where $\delta^{13}C$ of the ethane fraction is low relative to the methane and propane fractions. Alkanes with four or more carbons (C_{4+}) are present at trace levels in the McCully gases, making up no more than 1 vol %, and are considerably depleted in the FB samples relative to the HB (Table 2.1, Fig. 2.9). In all but one of the FB samples, the concentration of iso-butane is greater than n-butane, while the HB samples show the opposite trend, with concentrations of n-alkanes exceeding those of their branched isomers (Table 2.1, Fig. 2.10).

Table 2.1. Composition of gases from the McCully gas field

Well ID	Production unit[a,b]	CH_4 %vol	C_2H_6 %vol	C_3H_8 %vol	i-C_4 %vol	n-C_4 %vol	i-C_5 %vol	n-C_5 %vol	i-C_6 %vol	n-C_6 %vol	CO_2 %vol	O_2 %vol[c]	N_2 %vol
F-58	FB	93.29	1.44	0.60	-	0.037	-	-	-	-	0.078	-	4.68
F-58D	FB	93.62	1.51	0.08	0.003	0.001	-	0.001	-	-	0.087	0.076	4.95
E-67B	FB	94.52	2.02	3.26	0.009	0.006	-	0.001	-	0.002	0.052	-	0.38
J76	FB	88.01	2.59	6.93	0.017	0.009	-	-	-	-	0.006	0.917	2.12
J-76D	FB	88.38	2.63	7.30	0.021	0.012	-	-	-	-	0.006	-	2.07
P-76	FB	95.95	2.74	0.18	0.008	0.015	0.001	-	-	-	0.005	0.032	1.28
P-67	HB	93.30	4.91	1.11	0.086	0.194	0.040	0.058	0.004	0.012	0.005	0.032	0.57
C-57	HB	91.70	6.03	1.19	0.125	0.307	0.062	0.109	-	0.049	0.052	0.032	0.84
C-57D	HB	91.73	5.97	1.19	0.125	0.310	0.063	0.112	-	0.051	0.053	0.028	0.84
D-66	HB	0.62	0.05	0.57	0.043	0.117	0.046	0.095	0.046	0.019	0.033	-	94.16
G-67	HB	94.49	4.41	0.52	0.035	0.119	0.023	0.025	-	0.003	0.006	-	0.60
I-67	HB	90.79	6.31	1.56	0.193	0.466	0.091	0.159	0.027	0.047	0.015	0.032	0.86
J-38	HB	95.17	3.97	0.44	0.031	0.084	0.018	0.019	0.001	0.003	0.005	0.037	0.47
J-47	HB	93.09	4.96	1.08	0.137	0.302	0.067	0.095	0.016	0.029	0.006	0.032	0.59
K-48	HB	92.99	5.89	0.69	0.054	0.126	0.027	0.032	0.002	0.006	0.005	-	0.66
K-57	HB	93.27	4.96	0.95	0.112	0.243	0.053	0.078	0.016	0.027	0.006	0.049	0.57

a. FB: Frederick Brook shale unit

b. HB: Hiram Brook sandstone unit

c. O_2 concentrations are believed to represent atmospheric contamination

-. Below limit of detection

Na. Not measured

Table 2.1. (*continued*)

Well ID	$\delta^{13}C$ CH_4 (‰)	$\delta^{2}H$ CH_4 (‰)	$\delta^{13}C_2$ (‰)	$\delta^{2}H$ C_2 (‰)	$\delta^{13}C_3$ (‰)	$\delta^{2}H$ C_3 (‰)	$\delta^{13}C$ i-C_4 (‰)	$\delta^{2}H$ i-C_4 (‰)	$\delta^{13}C$ n-C_4 (‰)	$\delta^{2}H$ n-C_4 (‰)	$\delta^{13}C$ i-C_5 (‰)	$\delta^{2}H$ i-C_5 (‰)	$\delta^{13}C$ n-C_5 (‰)	$\delta^{2}H$ n-C_5 (‰)	$\delta^{13}C$ i-C_6 (‰)	$\delta^{2}H$ i-C_6 (‰)	$\delta^{13}C$ n-C_6 (‰)	$\delta^{2}H$ n-C_6 (‰)	$\delta^{13}C$ CO_2 (‰)	$\delta^{15}N$ N_2 (‰)
F-58	na	na	na	na	na	na	na	na	na	na	na	na	na	na	na	na	na	na	-17.3	na
F-58D	-32.5	-170.0	-37.2	-178.8	-36.9	-130.5	-41.0	-123.6	-37.5	-85.4	-	-	-	-	-	-	-	-	-19.4	-1.3
E-67B	-31.8	-159.4	-36.0	-177.0	-31.5	-123.5	-29.3	-	-34.3	-	-	-	-	-	-	-	-	-	-11.4	-3.8
J76	-34.9	-173.9	-38.3	-186.6	-31.3	-131.7	-28.3	-128.6	-34.9	-104.3	-	-	-	-	-	-	-	-	na	-3.2
J-76D	-34.8	-175.4	-38.3	-186.7	-31.3	-126.4	-28.4	-80.2	-35.1	-118.3	-	-	-	-	-	-	-	-	na	-3.0
P-76	-35.3	-167.5	-33.8	-182.4	-32.5	-172.5	na	na	na	na	na	na	na	na	na	na	na	na	na	-3.1
P-67	-36.0	-165.7	-34.4	-183.3	-30.7	-145.2	-	-	-	-	-	-	-	-	-	-	-	-	-	-2.2
C-57	-38.2	-171.7	-35.7	-176.6	-29.5	-160.7	-28.8	-133.4	-28.5	-143.9	-28.8	-133.7	-27.5	-144.7	-28.0	-130.7	-28.5	-	-31.7	-1.9
C-57D	-38.2	-169.7	-33.9	-178.7	-29.6	-157.6	-28.8	-130.3	-28.5	-143.8	-28.7	-131.3	-27.6	-137.3	-27.9	-129.2	-28.8	-	na	-1.9
D-66	na	na	na	na	na	na	na	na	na	na	na	na	na	na	na	na	na	na	na	na
G-67	-36.5	-167.9	-34.6	-181.2	-30.0	-160.5	-28.7	-135.3	-28.3	-140.8	-28.7	-135.3	-25.6	-133.4	nd	-119.2	-	-	na	-2.9
I-67	-39.4	-170.9	-33.7	-176.0	-30.0	-153.2	-29.4	-131.1	-28.8	-136.6	-28.6	-131.6	-28.2	-134.5	-28.4	-119.1	-28.7	-	na	-2.2
J-38	-34.4	-164.2	-36.4	-188.7	-33.4	-182.5	-29.9	-141.4	-31.0	-153.7	-29.8	-144.3	-26.5	-141.7	-27.2	-129.2	-28.3	-108	na	-0.9
J-47	-36.8	-163.9	-34.3	-179.3	-29.6	-161.0	na	na	na	na	na	na	na	na	na	na	na	na	na	-1.6
K-48	-37.0	-168.6	-35.4	-178.5	-29.5	-157.9	-27.3	-132.7	-28.3	-145.2	-26.6	-130.3	-25.7	-126.7	-26.3	-98.9	-25.0	-	na	-0.4
K-57	-36.2	-168.7	-34.3	-188.5	-28.6	-154.7	na	na	na	na	na	na	na	na	na	na	na	na	na	-1.4

Figure 2.5. Bernard plot of the McCully gas field samples (Bernard et al. 1976). The methane fractions of the deeper FB samples show a trend of ^{13}C enrichment while dryness (C_1/C_2+C_3) is variable.

Figure 2.6. Schoell plot of the McCully gas field samples (Schoell, 1983). All samples fall within the thermogenic window, and a general trend of ^{13}C enrichment with ^{2}H is apparent among the HB and some FB samples.

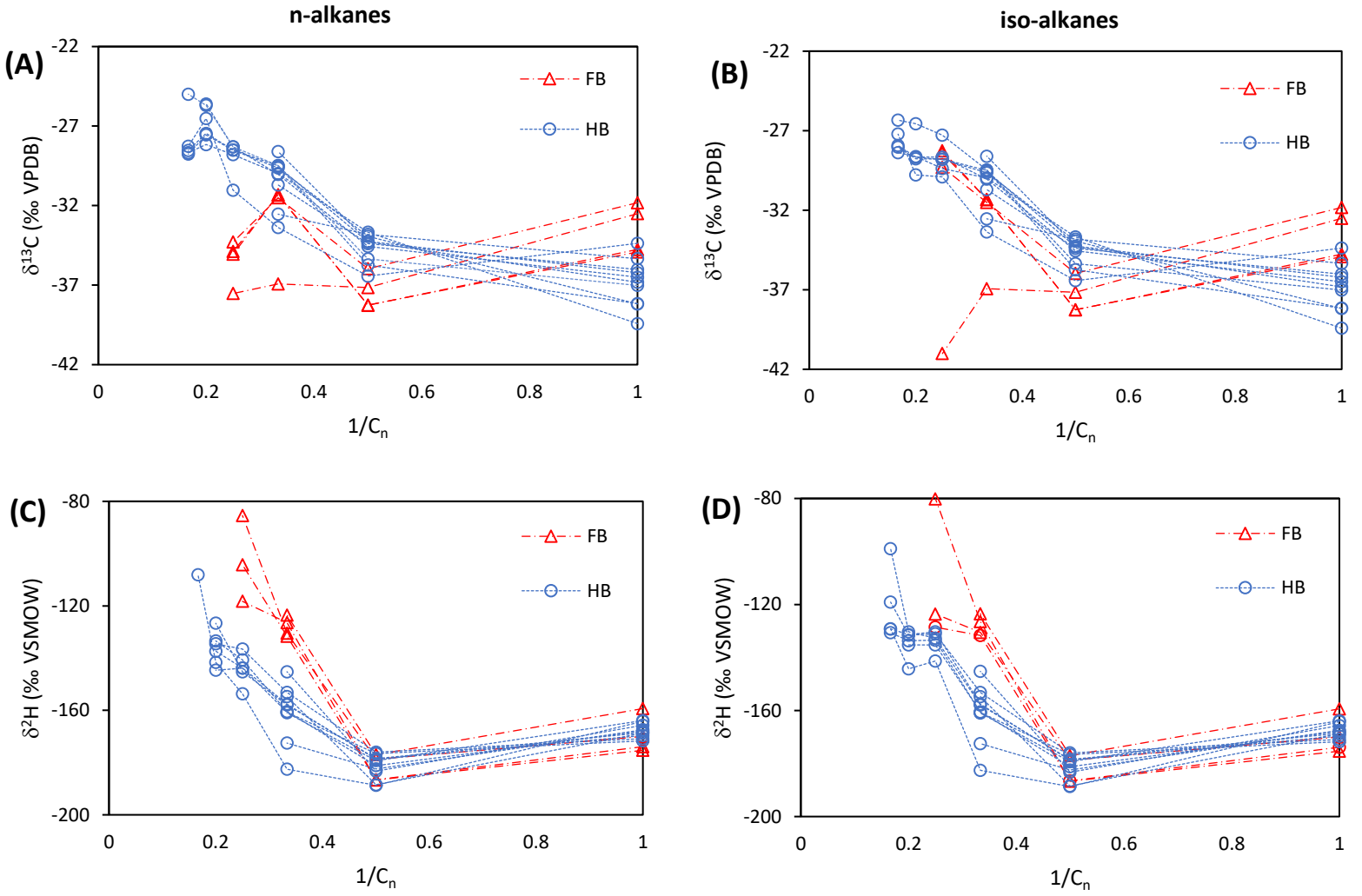

Figure 2.7. Natural gas plots of the McCully gas field samples (Chung et al. 1988). (A) $\delta^{13}C$ n-alkanes, (B) $\delta^{13}C$ iso-alkanes, (C) $\delta^{2}H$ n-alkanes, (D) $\delta^{2}H$ iso-alkanes. $1/C_n$ refers to the reciprocal carbon number of each hydrocarbon fraction (eg: $C_{n\text{-methane}} = 1$, $C_{n\text{-ethane}} = 1/2$, $C_{n\text{-propane}} = 1/3$, etc).

Deuterium isotopic profiles of the FB and HB samples also display V-shaped trends, with ^{2}H in the ethane fractions depleted relative to the methane and propane fractions ($\delta^{2}H$-C_1>$\delta^{2}H$-C_2<$\delta^{2}H$-C_3) (Fig. 2.7 C,D). As with the carbon isotope profiles (Fig. 2.7 A,B), differences in $\delta^{2}H$ are apparent between the n- and iso-alkanes of the C_{4-6} fractions. These differences are particularly apparent in the FB samples, in which $\delta^{2}H$ values differ by as much as 38‰ between the n- and iso-butane fractions, while the n- and iso-butane, pentane, and hexane fractions of the HB samples are similar to one another within the limits of analytical uncertainty.

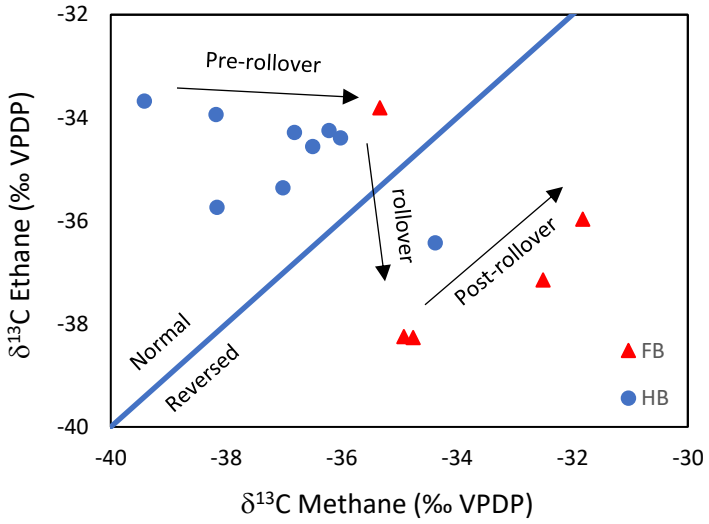

Figure 2.8. Plot of $\delta^{13}C_{methane}$ versus $\delta^{13}C_{ethane}$ (Tilley et al. 2011) for the McCully field natural gas samples.

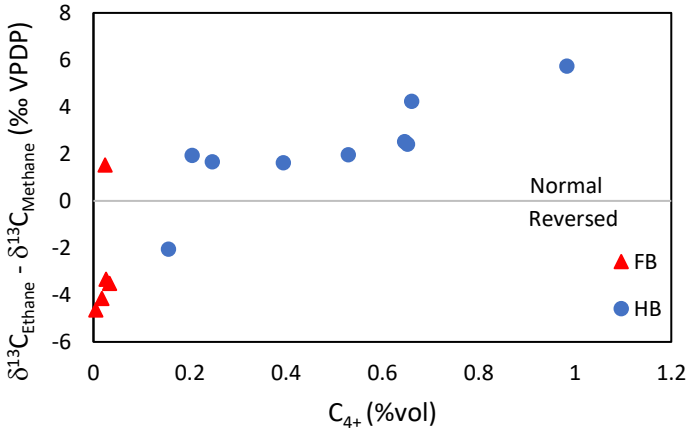

Figure 2.9. Plot of C_{4+} concentrations (vol %) versus $\delta^{13}C_{Ethhane}$ - $\delta^{13}C_{Methane}$ of the McCully samples.

The occurrence of isotopically reversed natural gas in unconventional reservoirs appears to be closely related to reservoir maturity, elevated gas dryness, and divergence of reservoir fluid pressures from local gradients, generating overpressured domains in the gas-rich units; the most widely accepted conceptual model explaining the occurrence of these gases is that at elevated stages of reservoir maturity, longer chain hydrocarbons (C_{2-5}) which are enriched in ^{13}C, become unstable and decompose to produce ^{13}C enriched methane (Zumberge et al. 2012;

Chatellier et al. 2013; Tilley and Muelenbachs, 2013). This process is thought to occur only under elevated reservoir temperature and pressure conditions, and may require the presence of water. Under this model, the extremely low permeability of unconventional reservoirs acts to trap early produced hydrocarbons in place, where they are exposed to progressively increasing pressures and temperatures. When the stability fields of the longer chain hydrocarbons are exceeded, they decompose to produce more thermodynamically stable compounds, ultimately forming methane. This process raises gas dryness along with reservoir pressure as the volume of methane increases, and ultimately results in an isotopic reversal (Burruss and Laughrey 2010; Zumberge et al. 2012; Chatellier et al. 2013; Golding et al. 2013; Tilley and Muelenbachs, 2013). This process may also affect the relative proportions of n- and iso-alkanes, if the 'normal' isomers decompose at a higher rate than their more thermodynamically stable, branched isomers (McKee et al. 2013).

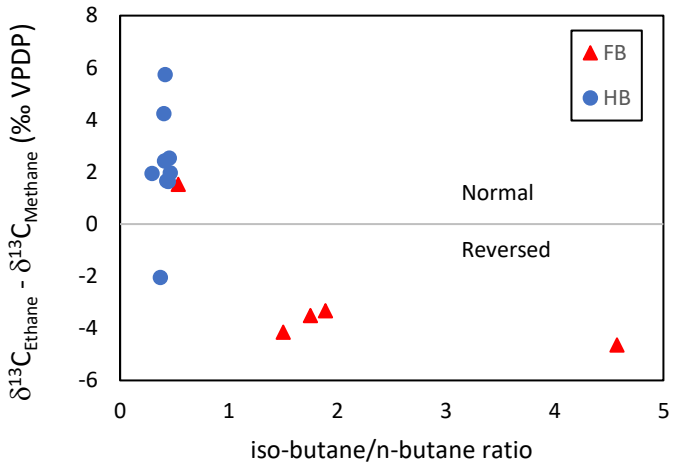

Figure 2.10. Plot of $\delta^{13}C_{methane}$ - $\delta^{13}C_{ethane}$ (‰ VPDP) versus iso-butane/n-butane concentration ratios of the McCully gas samples. The samples show a trend of increasing iso-butane/n-butane as the methane-ethane δ^{13} differential

In order to better understand this process, it is useful to consider observations from unconventional gas fields alongside the results of laboratory kerogen and oil cracking experiments, which have provided key insights into the process of natural gas generation. These experiments have shown that 1) under closed system conditions at elevated pressures and temperatures, C_{2-5} hydrocarbons will, as predicted, decompose to form $\delta^{13}C$ enriched methane (Behar et al. 1992; Hill et al, 2003), 2) this process is greatly enhanced by the presence of water

(Gao et al. 2014), and 3) full isotopic reversals can be achieved at extremely high P and T conditions (500-700 ^{o}C, 1-3 GPa, for 120 min) (Du et al, 2003). The V-shaped trend of δ^{13}C enrichment in methane and propane relative to ethane that is seen in the McCully samples (Fig. 2.7 A,B), was also observed in natural gas produced in laboratory cracking experiments by Hill et al. (2003). In their experiments, longer chain hydrocarbons enriched in ^{13}C, decomposed to methane and propane, enriching their δ^{13}C values relative to that of ethane after extended periods of cracking under high-pressure, in closed-system conditions.

In their comprehensive review of the stable isotope geochemistry of unconventional petroleum systems in Canada and the United States, Tilley and Muehlenbachs (2013) described three stages of natural gas maturation in sealed, self-contained reservoirs: the pre-rollover, rollover, and post-rollover zones. Gases from both the HB sandstone and FB shale appear to follow this same general trend, with most of the FB samples falling into the rollover or post-rollover zones and the HB samples falling into the pre-rollover and rollover zones (Fig. 2.8). Due to variable and elevated propane concentrations in some of the FB samples, there are no clear trends with regards to gas dryness. However, a correlation does exist between the concentrations of C_{4+} fractions (butane-hexane) and the δ^{13}C differential between methane and ethane (Fig. 2.9). This trend may indicate that conditions within the FB reservoir were more favourable for the cracking of longer chain hydrocarbons and isotopic rollover than in the HB. In a trend similar to what was observed by Zumberge et al, (2012) in gas from the Barnett shale, the ratio of iso-/n-butane in the McCully gases appears to increase with maturity and isotope reversal (Fig. 2.10), possibly reflecting greater stability of the branched alkanes relative to their normal isomers under elevated temperature and pressure conditions. However, unlike gas from the

Barnett, iso-/n-butane ratios for the McCully gasses do not decrease sharply in the most mature samples, instead they appear to simply increase. This difference may be due to geochemical differences between the two reservoirs, possibly indicating that the most mature samples from the McCully field are still less mature than those of the Barnett, or it may simply be due to the relatively small data set from the McCully field.

In their study of unconventional natural gas reservoirs in the Appalachian basin, Burruss and Laughrey (2010) concluded that isotopic reversals cannot be accounted for by wet gas cracking alone. The increase in $\delta^{13}C$ of the methane fractions in isotopically reversed gasses may be explained by the generation of ^{13}enriched methane from late cracking of the ^{13}C enriched C_{2-5} hydrocarbon fractions, which are found at considerably reduced concentrations in isotopically reversed gasses compared to less mature gasses from the same fields. However, wet gas cracking cannot account for the ^{13}C depletion that is observed in the C_{2-4} fractions which is a characteristic of fully isotopically reversed gasses. Burruss and Laughrey (2010) propose a series of reactions involving hydrocarbons with water and transition metals, affected by Rayleigh fractionation, which in addition to the generation of ^{13}C enriched methane generated by wet gas cracking, may provide a more complete understanding of the processes which cause isotopic reversal of natural gas in unconventional reservoirs. The same conclusion may likely be drawn for the McCully gasses, which show a clear trend of decreasing C_{4+} concentrations with increasing maturity and isotopic reversal (Fig 2.9). The depleted $\delta^{13}C$ values of the ethane and butane fractions of the isotopically reversed samples however can only be explained if additional reaction pathways such as those described by Burruss and Laughrey (2010) are considered.

Composition of natural gas differs significantly between the FB and HB, considering that the kerogen sources for both reservoirs are essentially equivalent, such differences in chemical and isotopic composition can only be explained by the physical conditions under which gas was generated. Physically, the FB shale is similar to the gas-bearing shales which have been the target of major development throughout the United States and western Canada, essentially a kerogen-rich unit with extremely low permeability that is able to act as both a source-rock and reservoir for natural gas. Once kerogen in the FB shale began to crack, hydrocarbons were likely trapped in place where they accumulated and were subjected to increasing temperatures and pressures during subsidence of the Albert Formation. Under effectively closed-system conditions, longer chain hydrocarbons produced early in the cracking process became unstable, leading to secondary cracking, and evolution toward isotopic profiles in which ^{13}C is enriched in methane and depleted ethane and propane (Tilley and Muelenbachs, 2013). Hydrocarbons found in the overlying HB sandstone were likely generated in the interbedded shales along with some small amount of migration from the underlying FB shale. Because the HB sandstone is less of a closed system, the conditions required to mature natural gas to the point of isotopic reversal were likely not fully achieved. As a result, gas in the HB is less mature and displays only the initial stages of isotopic rollover.

2.4.2 Produced water

Compositions of the produced waters from the McCully field are dominated by sodium and chloride, with salinities between 2,070 and 53,650 mg/kgw (Table 2.2). For comparison, the salinity of seawater is typically between 30,000 and 35,000 mg/kgw. The Na/Cl ratios for most samples fall close to that of seawater, while the Br/Cl ratios are more variable, showing both

depletion and enrichment of Br relative to seawater. The non-conservative ions Mg, K, and S are depleted relative to chloride compared to seawater, while Ca is enriched in most samples (Fig 2.11). The produced waters display trends which are typical of seawater that has been affected by diagenetic reactions. The Na/Cl, and Br/Cl ion ratios of several samples are distinctly marine while others show enrichment and depletion of Na and Br. The enriched Ca and depleted Mg, SO_4, and K/Cl ratios are typical of seawater that has been affected by dolomitization of carbonates, sulfate reduction and clay-mineral reactions respectively (Clayton et al 1966; Carpenter, 1978; Stueber et al. 1993).

Stable isotope analysis of the water samples ($\delta^{18}O$ and $\delta^{2}H$) show that all but one plot to the right of the Global Meteoric Water Line (GMWL), with most displaying similar $\delta^{2}H$ values to shallow groundwater from the gas field. The stable isotope compositions of several samples plot along a trajectory which intersects with local shallow groundwater samples on the GMWL (Fig. 2.12). This pattern has been reported in other oil and gas field waters which are believed to have been influenced by meteoric infiltration (Clayton et al. 1966; Hitchson and Friedman, 1969; Kharaka et al. 1973, 1979). Strontium isotope ratios of the McCully waters are considerably enriched in radiogenic ^{87}Sr relative to modern and Mississippian seawater (Burke et al, 1982).

Table 2.2. Major Ion and Isotope Composition of Produced Water Samples

ID	Production unit	δ^2H (‰)[a]	$\delta^{18}O$ (‰)[b]	TDS mg/kgw	Na mg/kgw	Mg mg/kgw	K mg/kgw	Ca mg/kgw	S[c] mg/kgw	Sr mg/kgw	Fe mg/kgw	Cl mg/kgw	Br mg/kgw	I mg/kgw	CaCO3 mg/kgw	$^{87}Sr/^{86}Sr$[d]
F-58	FB	-158.6	-14.1	2070.1	629.9	10.3	7.2	18.3	42.2	0.8	-	1050.3	4.5	1.7	305	0.7111
E-67	FB	-69.6	-2.9	34589.1	10147.0	533.9	325.7	411.1	133.1	57.9	47.2	22361.4	44.0	7.8	520	0.7117
J-76	FB	-49.3	-2.5	44680.7	14191.3	900.6	668.0	660.1	268.1	140.2	144.3	27241.7	40.9	5.4	420	0.7121
C-57	HB	-59.1	-5.5	25579.8	7017.4	149.3	42.9	895.1	184.2	509.6	-	16201.3	39.3	5.8	535	0.7100
I-67	HB	-108.1	-7.5	20440.5	6322.2	110.0	43.7	501.6	42.5	8.6	-	12918.3	37.9	5.6	450	0.7099
J-38	HB	-55.9	0.0	53646.1	17861.1	179.9	123.2	532.9	182.3	8.3	-	34562.1	82.2	14.2	100	0.7107
J-47	HB	-59.5	-3.9	32808.6	10452.9	270.6	141.8	923.0	545.1	31.0	10.1	20161.6	197.4	10.2	65	0.7108
K-48	HB	-141.5	-23.2	23190.1	8005.7	61.9	282.1	158.4	151.0	27.2	-	14374.6	54.7	4.4	70	0.7105
K-57	HB	-53.6	-2.6	32631.9	10149.7	108.8	70.7	723.3	13.9	591.3	146.0	20769.7	52.0	6.6	0	0.7099

a. δ^2H measured relative to VSMOW

b. $\delta^{18}O$ measured relative to VSMOW

c. S measured as elemental sulfur by ICP-OES

d. $^{87}Sr/^{86}Sr$ measured relative to NBS987 ± 0.000020‰

-. Measurement below limit of detection

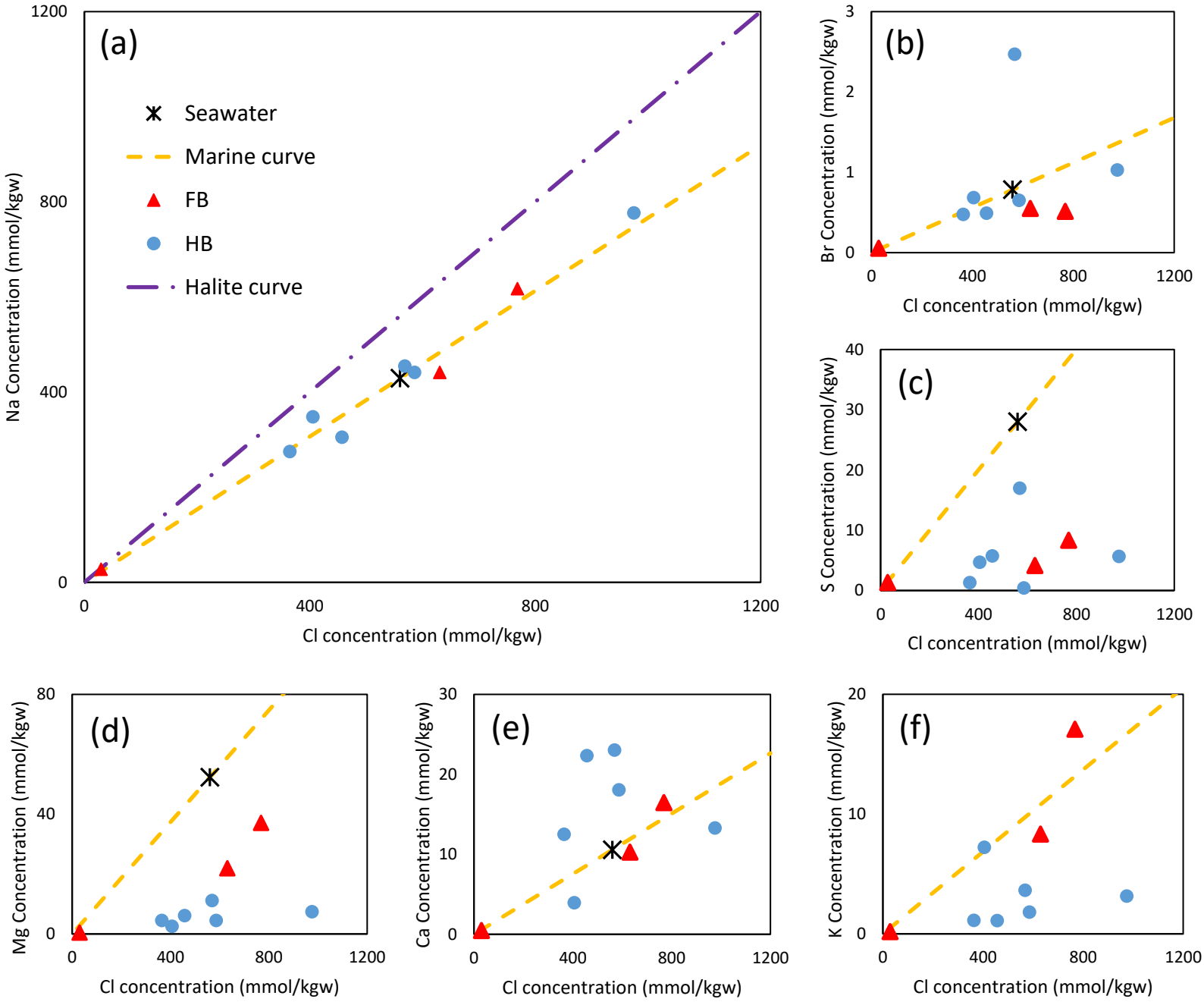

Figure 2.11. Chloride normalized cross plots of (A) sodium, (B) Bromide, (C) elemental sulfur, (D) magnesium, (E) calcium, (F) potassium. McCully production water samples are plotted relative to marine water evaporation/dilution curves and seawater. The "Marine curves" are plotted using the measured ion ratio of the seawater reference standard in order to account for possible measurement bias.

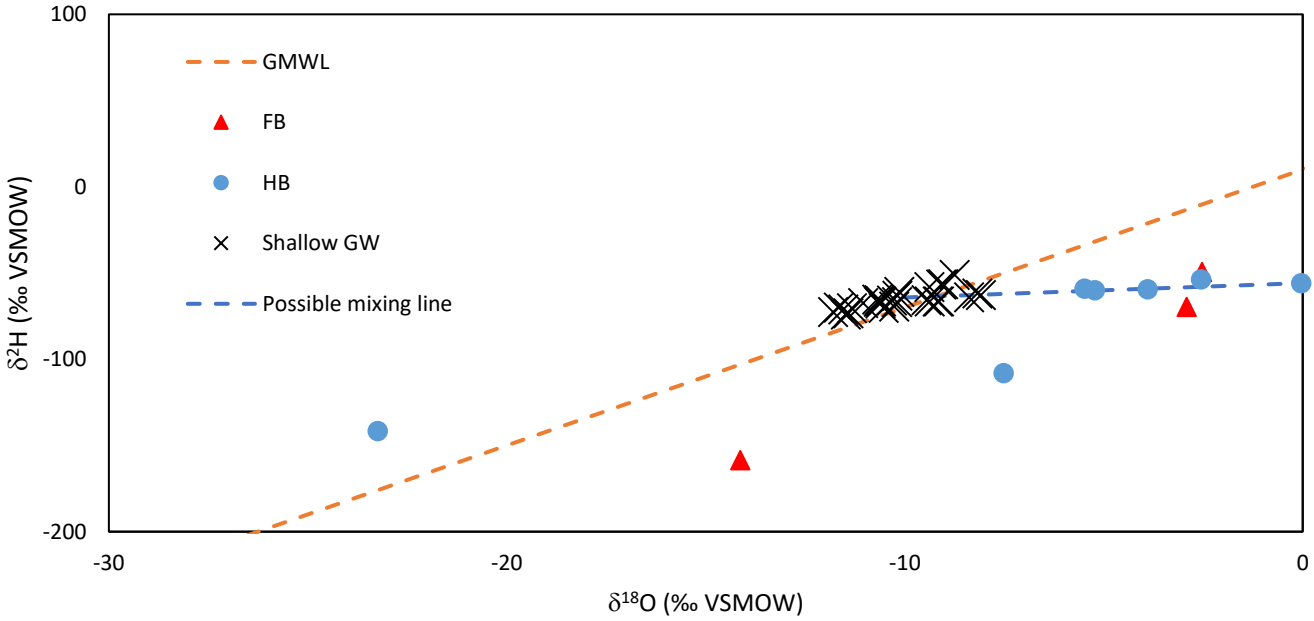

Figure 2.12. Cross plot of δ^2H and $\delta^{18}O$ of the McCully production waters and shallow groundwater from the McCully area relative to the global meteoric water line (GMWL). A possible mixing line connects selected production water samples with shallow groundwater.

Interpretation of the produced water samples is complicated by two factors, 1) the precipitates which formed after the samples were collected, and 2) the close relationship between salinity and $\delta^{18}O$ (Fig. 2.13). A SEM-EDS analysis of the precipitates revealed the presence of sulfur, oxygen and iron with small quantities of silicon, aluminium, and calcium. While the formation of these precipitates undoubtedly resulted in significant alteration of water chemistry with respect to sulfur, iron, and trace metals, it is unlikely that the concentrations or ratios of major ions, specifically those of Na, Cl, and Br were significantly affected. The relationship observed between salinity and $\delta^{18}O$ is a strong indication that the produced waters

have been influenced by the effects of refluxing within the production wells, a process which results in condensation and mixing of water vapour at the wellhead (Khakara et al. 1985).

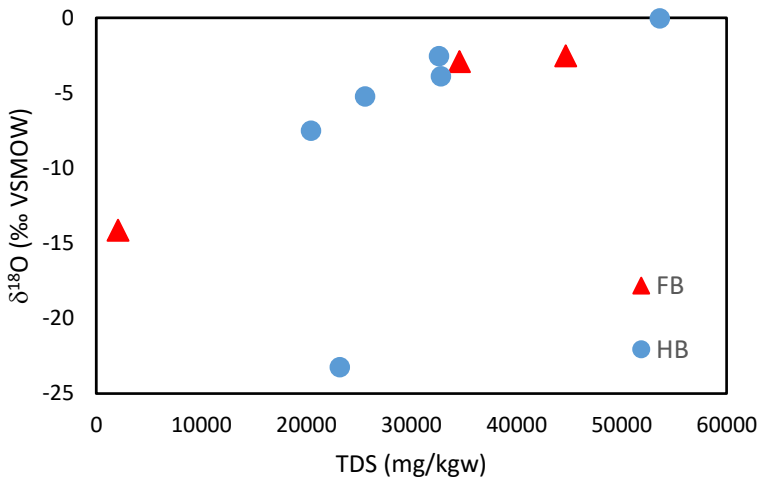

Figure 2.13. Cross plot of $\delta^{18}O$ and total dissolved solids (TDS) (mg/kgw) for the McCully production water samples.

The salinity of deep formation waters can vary greatly between, and within sedimentary basins, from concentrations as low as 510 mg/L in the evaporite-free San Joaquin Basin in California (Fisher and Boles, 1989) to concentrations in excess of 600,000 mg/L in the evaporite-rich Michigan Basin (Case, 1945). The major-ion composition of formation waters in oil and gas fields is typically Na-Cl dominated, although highly saline Na-Ca-Cl type brines have also been reported (Lowenstein et al. 2003; Kharaka and Hanor, 2003). Enrichment of radiogenic strontium, which is common in deep sedimentary basin formation waters, is believed to result from ion exchange with silicate minerals as well as ingrowth of ^{87}Sr form radioactive decay of ^{87}Rb over geologic time (McNutt et al. 1987; Stueber et al. 1993). While the high salinities and marine-like ionic compositions of deep formation waters are generally thought to reflect the influence of connate seawater (White et al. 1963; Carpenter, 1978), the application of stable isotope geochemistry has demonstrated that formation waters often have complex hydrogeologic histories, often involving mixing from multiple sources including local meteoric waters (Clayton et al, 1966; Kharaka and Hanor, 2004; Rostron and Arkadaskskiy, 2014). However, as is seen in the McCully samples, the application of stable isotope methods can be complicated by the tendency of water produced from natural gas

wells to differ in chemical and isotopic composition from true formation water due to the effects of isotope fractionation and dilution when water vapour, co-produced with natural gas, condenses at the well head and mixes with produced water (Khakara et al. 1985). The extent of dilution depends on reservoir conditions such as temperature and pressure, as well as formation water salinity, all of which affect the partial pressure of water vapour in the production well. This issue is often resolved by culling data from wells with excessively low water/gas production ratios.

Major ion chemistry of the produced water samples suggests that the salinity of formation water in the McCully gas field is likely derived from connate marine water which has undergone alteration through water-rock and diagenetic reactions including dolomitization, sulfate reduction, and clay-mineral reactions. Evidence of these reactions is present in the mineralogical record of the Albert Formation, where abundant dolomite cements and pyrite have been reported (Choudhry and Noble, 1996). There is some variation between the Na/Cl and Br/Cl ratios of the produced waters and marine water, however these variations do not show any systematic trend which would indicate influence from another salinity source such as halite or seawater bitterns. The enrichment of radiogenic strontium in the waters is an indication of a long residence time and interaction with silicate minerals.

Considering that the rocks of the Albert Formation are believed to be entirely of continental origin, and are well separated from the marine strata of the Windsor Group, the most likely explanation for the salinity observed today is basin-scale fluid circulation. Denser, saline water may have migrated downward from the overlying sea which was present during the deposition of the Windsor Group. Considering that the salinity of produced waters from the

McCully field appears to be marine with no evidence of influence by seawater bitterns or halite dissolution, the downward migration of water must have occurred prior to both the marine regression which deposited the evaporites of the Windsor group, and the over-pressurization of the HB and FB Members resulting from hydrocarbon generation.

The stable oxygen and hydrogen isotope ratios of several produced water samples fall along a line which intersects the GMWL at the location of shallow groundwater from the gas field. This trend may reflect local meteoric water influence in the reservoir, possibly related to the drilling and hydraulic fracturing of production wells. However, interpretation of these results is complicated by the linear relationship between ^{18}O and salinity of the production water samples, which may indicate that refluxing and wellhead condensation have altered the composition of formation water during production. Unfortunately, due to the small number of samples, and due to the fact that production wells in the McCully field contain multiple perforations across several hundred meters of vertical depth, it is not possible to draw any detailed conclusions regarding the origin and nature of formation water in the Albert formation with the available isotopic data.

2.5 Conclusions

Chemical and stable isotope analyses of production gas and water from tight shale and sandstone reservoirs in the McCully gas field, reveal a complex history of fluid migration and mixing as well as hydrocarbon generation and maturation. Natural gas in the FB shale appears to have undergone an isotopic rollover to the extent of a full isotopic reversal. This is likely the result of secondary cracking of liquid hydrocarbons under elevated temperature and pressure conditions within the extremely low permeability shale reservoir. Gas in the overlying HB

sandstone similarly shows evidence of isotopic rollover, but to a lesser extent likely due to slightly higher permeability. Evidence of isotopic rollover and reversal in the FB shale reservoir may have significant implications regarding its economic potential, as the occurrence of isotopically reversed gas has been associated with notably high rates of productivity and low rates of decline in other shale gas reservoirs (Zumberge et al. 2012). Major ion chemistry of the produced waters from the McCully field indicate a connate marine source which may have been influenced by meteoric water. Considering the terrestrial nature of the Albert Formation, the most plausible explanation for the marine-like water found in it today, is downward migration during the late-Mississippian marine incursion during which the Windsor Group was deposited.

2.6 Conceptual Model

Based on the results of this study, a basic conceptual model has been developed describing the geochemical evolution of fluids in the McCully gas field.

1. Deposition of the Albert Formation sediments. Composition of porewater in the sediments at the time likely reflected the fluvial and lacustrine environments in which they were deposited.
2. Deposition of the Sussex Group, followed by the Windsor Group during a marine incursion into the Moncton basin. During the marine incursion, dense marine water began circulating downward through the Sussex and Horton Groups, undergoing alteration from an initial seawater composition due to diagenetic processes such as dolomitization, sulfate reduction, and clay-mineral reactions. The altered marine water infiltrated permeable strata in the Albert Formation, displacing connate water of lower salinity in the HB and likely mixing by diffusion with connate water near the boundary with the lower-permeability FB member.

3. Thermal cracking of organic matter in the Albert Formation resulting in the generation of natural gas raised fluid pressure within the formation, preventing further infiltration of fluids.
4. Following thermogenic natural gas generation in the Albert Formation, processes which likely included a combination of wet-gas cracking and reactions involving hydrocarbons with water and transition metals result in full and partial isotopic reversal of natural gas in the FB and partial isotopic rollover in the HB.

2.7 References Cited

Al, T.A., Leblanc, J., and Phillips, S. (2013). A study of Groundwater Quality from Domestic Wells in the Sussex and Elgin Region, New Brunswick: with Comparison to Deep Formation Water and Gas from the McCully Gas Field.; Geological Survey of Canada, Open File 7449, 40p. doi:10.4095/292762

Behar, F., Kressmann, S., Rudkiewicz, J. L., & Vandenbroucke, M. (1992). Experimental simulation in a confined system and kinetic modelling of kerogen and oil cracking. *Organic Geochemistry*, *19*(1-3), 173-189.

Bernard, B. B., Brooks, J. M., & Sackett, W. M. (1976). Natural gas seepage in the Gulf of Mexico. *Earth and Planetary Science Letters*, *31*(1), 48-54.

Burke, W. H., Denison, R. E., Hetherington, E. A., Koepnick, R. B., Nelson, H. F., & Otto, J. B. (1982). Variation of seawater 87Sr/86Sr throughout Phanerozoic time. *Geology*, *10*(10), 516-519.

Burruss, R. C., & Laughrey, C. D. (2010). Carbon and hydrogen isotopic reversals in deep basin gas: Evidence for limits to the stability of hydrocarbons. *Organic Geochemistry*, *41*(12), 1285-1296.

Case, L. C. (1945). Exceptional Silurian brine near Bay City, Michigan. *AAPG Bulletin*, *29*(5), 567-570.

Chatellier, J. Y., Flek, P., Molgat, M., Anderson, I., Ferworn, K., Larsen, N. L., & Ko, S. (2013). Overpressure in shale gas: When geochemistry and reservoir engineering data meet and agree.

Chowdhury, A. H., Fowler, M. G., & Noble, J. P. (1991). Petroleum geochemistry and geology of the Albert Formation Moncton Subbasin, New Brunswick, Canada. *Bulletin of Canadian Petroleum Geology*, *39*(4), 315-331.

Connolly, C. A., Walter, L. M., Baadsgaard, H., & Longstaffe, F. J. (1990). Origin and evolution of formation waters, Alberta basin, western Canada sedimentary basin. I. chemistry. *Applied Geochemistry*, *5*(4), 375-395.

Carpenter, A. B. (1978, January). Origin and chemical evolution of brines in sedimentary basins. In *SPE Annual Fall Technical Conference and Exhibition*. Society of Petroleum Engineers.

Chowdhury, A. H., & Noble, J. P. (1996). Organic carbon and pyrite sulphur relationships as evidences of bottom water conditions of sedimentation, Albert Formation fine-grained lacustrine sediments, New Brunswick, Canada. *Marine and Petroleum Geology*, *13*(1), 79-90.

Chung, H. M., Gormly, J. R., & Squires, R. M. (1988). Origin of gaseous hydrocarbons in subsurface environments: theoretical considerations of carbon isotope distribution. *Chemical Geology*, *71*(1-3), 97-104.

Clayton, R. N., Friedman, I., Graf, D. L., Mayeda, T. K., Meents, W. F., & Shimp, N. F. (1966). The origin of saline formation waters: 1. Isotopic composition. *Journal of Geophysical Research*, *71*(16), 3869-3882.

Corridor Resources. (2017, Aug). *Corporate presentation.* Retrieved from https://www.corridor.ca/your-investment/events-presentations/

Dai, J., Ni, Y., Gong, D., Feng, Z., Liu, D., Peng, W., & Han, W. (2017). Geochemical characteristics of gases from the largest tight sand gas field (Sulige) and shale gas field (Fuling) in China. *Marine and Petroleum Geology*, *79*, 426-438.

Du, J., Jin, Z., Xie, H., Bai, L., & Liu, W. (2003). Stable carbon isotope compositions of gaseous hydrocarbons produced from high pressure and high temperature pyrolysis of lignite. *Organic Geochemistry*, *34*(1), 97-104.

EPA. (2017, Jan 9). *The process of hydraulic fracturing.* Retrieved from https://www.epa.gov/hydraulicfracturing/process-hydraulic-fracturing

Ferworn, K., Zumberge, J. Reed, J., Brown, S. (2008). *Gas character anomalies found in highly productive shale gas wells*: Geomark Research Huston, Texas, USA, Accessed 07/17/17 http://www.zenzebra.net/quebec/Ferworn_et_al_2008.pdf

Fisher, J. B., & Boles, J. R. (1990). Water—rock interaction in Tertiary sandstones, San Joaquin basin, California, USA: Diagenetic controls on water composition. *Chemical Geology*, *82*, 83-101.

Gao, L., Schimmelmann, A., Tang, Y., & Mastalerz, M. (2014). Isotope rollover in shale gas observed in laboratory pyrolysis experiments: Insight to the role of water in thermogenesis of mature gas. *Organic Geochemistry*, *68*, 95-106.

Golding, S. D., Boreham, C. J., & Esterle, J. S. (2013). Stable isotope geochemistry of coal bed and shale gas and related production waters: a review. *International Journal of Coal Geology*, *120*, 24-40.

Government of New Brunswick. (2017). *Geology of sedimentary basins*. Retrieved from http://www2.gnb.ca/content/gnb/en/departments/erd/energy/content/minerals/content/Geology_SedimentaryBasins.html

Government of New Brunswick. (2018a). *Distribution of subbasins and uplifts in the Maritimes Basin*. Retrieved from http://www2.gnb.ca/content/dam/gnb/Departments/en/images/Carbon_2-e.jpg

Government of New Brunswick. (2018b). *Maritimes basin*. Retrieved from http://www2.gnb.ca/content/dam/gnb/Departments/en/images/Maritimes_Basin_Chart.jpg

Government of New Brunswick. (2018c). *Hydrocarbon occurrences*. Retrieved from http://www2.gnb.ca/content/dam/gnb/Departments/en/images/Carbon_7-e.jpg

Government of New Brunswick. (2018d). *McCully gas field*. Retrieved from http://www2.gnb.ca/content/dam/gnb/Departments/en/images/Carbon_6-e.jpg

Gussow, W. C. (1953). Carboniferous stratigraphy and structural geology of New Brunswick, Canada. *AAPG Bulletin*, *37*(7), 1713-1816.

Hill, R. J., Tang, Y., & Kaplan, I. R. (2003). Insights into oil cracking based on laboratory experiments. *Organic Geochemistry*, *34*(12), 1651-1672.

Hinds, S.J., St. Peter, C.J., (2006). Stratigraphy and structure of the Moncton Subbasin in the Urney–Waterford area, Maritimes Basin, New Brunswick: implications for the McCully Natural Gas Field. *In* Geological Investigations in New Brunswick for 2005. Edited by G.L. Martin, New Brunswick Department of Natural Resources; Minerals, Policy and Planning Division, Mineral Resource Report 2006-3, p.73-102.

Hinds, S., St. Peter, C., (2016). The McCully gas field project. Department of natural resources Geological surveys branch, New Brunswick, 17p. See website http//www2.gnb.ca/content/dam/gnb/80Departments/en/pdf/Minerals-minerales/McCully_Gas_Field_Project-e.pdf (accessed online on March 30, 2016).

Hitchon, B., & Friedman, I. (1969). Geochemistry and origin of formation waters in the western Canada sedimentary basin—I. Stable isotopes of hydrogen and oxygen. *Geochimica et Cosmochimica Acta*, *33*(11), 1321-1349.

Keighley, D. (2008). A lacustrine shoreface succession in the Albert Formation, Moncton Basin, New Brunswick. *Bulletin of Canadian Petroleum Geology*, *56*(4), 235-258.

Keighley, D., & St Peter, C. (2006). Selected core from the Albert Formation (Mississippian) Moncton Basin, Southern New Brunswick. In *Canadian Society of Petroleum Geologists CSPG Convention 2006. Extended abstracts volume* (pp. 605-615).

Kharaka, Y. K., Berry, F. A., & Friedman, I. (1973). Isotopic composition of oil-field brines from Kettleman North Dome, California, and their geologic implications. *Geochimica et Cosmochimica Acta*, *37*(8), 1899-1908.

Kharaka, Y. K., Lico, M. S., Wright, V. A., & Carothers, W. W. (1980, June). Geochemistry of formation waters from Pleasant Bayou No. 2 well and adjacent areas in coastal Texas. In *Texas Univ. Bureau Economics Geology, US Gulf Coast Geopressured-Geothermal Energy Research and Development Conference;(United States)* (Vol. 1).

Kharaka, Y. K., Hull, R. W., & Carothers, W. W. (1985). Water-rock interactions in sedimentary basins. *Relationship of organic matter and mineral diagenesis: SEPM Short Course*, *17*, 79-176.

Kharaka, Y. K., & Hanor, J. S. (2003). Deep fluids in the continents: I. Sedimentary basins. *Treatise on geochemistry*, *5*, 605.

LeBlanc, D., Huskins, L., & Lestz, R. (2011). Propane-based fracturing improves well performance in Canadian tight reservoirs. *World oil*, *232*(7).

Lowenstein, T. K., Hardie, L. A., Timofeeff, M. N., & Demicco, R. V. (2003). Secular variation in seawater chemistry and the origin of calcium chloride basinal brines. *Geology*, *31*(10), 857-860.

Martel, T., & Durling, P. (2001). The petroleum geology of the McCully# 1 gas discovery. *Atlantic geology*. 37(1), 118.

McKee, W. C., & Schleyer, P. V. R. (2013). Correlation Effects on the Relative Stabilities of Alkanes. *Journal of the American Chemical Society*, *135*(35), 13008-13014.

McNutt, R. H., Frape, S. K., & Dollar, P. (1987). A strontium, oxygen and hydrogen isotopic composition of brines, Michigan and Appalachian Basins, Ontario and Michigan. *Applied Geochemistry*, *2*(5-6), 495-505.

NRCan. (2016a, Aug 23). *Shale and tight resources in Canada.* Retrieved from http://www.nrcan.gc.ca/energy/sources/shale-tight-resources/17669

NRCan. (2016b, Aug 23). *Exploration and production of shale and tight resources.* Retrieved from http://www.nrcan.gc.ca/energy/sources/shale-tight-resources/17677

NRCan. (2017a, Jul 25). *New Brunswick`s shale and tight resources.* Retrieved from http://www.nrcan.gc.ca/energy/sources/shale-tight-resources/17698

NRCan. (2017b, Oct 11). *Natural gas facts.* Retrieved from http://www.nrcan.gc.ca/energy/facts/natural-gas/20067

Park, F. A. (2014). Shale gas in New Brunswick: geological background. In Saillant, R & Campbell, D (Eds.), *Shale gas in New Brunswick towards a better understanding.* Moncton, NB: Canadian institute for research on public policy and public administration.

Perrin, J., & Cook, T. (2016, May 5). *Hydraulically fractured wells provide two thirds of U.S. natural gas production.* Retrieved from https://www.eia.gov/todayinenergy/detail.php?id=26112

Rivard, C., Lavoie, D., Lefebvre, R., Séjourné, S., Lamontagne, C., & Duchesne, M. (2014). An overview of Canadian shale gas production and environmental concerns. *International Journal of Coal Geology*, *126*, 64-76.

Rivard, Lavoie, D., Pinet, N., Duchesne, M.J., Bordeleau, G., Séjourné, S., Huchet, F., Lefebvre, R., Brake, V., Crow, H., Malet, X. (2017). A study of aquifer vulnerability to hydrocarbon development in southern New Brunswick, conference proceedings, GeoOttawa 2017, 70th Canadian Geotechnical Conference and the 12th Joint CGS/IAH-CNC Groundwater Conference, October 1-4 2017, Ottawa, Canada.

Rostron, B., & Arkadakskiy, S. (2014). Fingerprinting "Stray" Formation Fluids Associated and Production with Hydrocarbon Exploration and Production. *Elements*, *10*(4), 285-290.

Séjourné, S. (2017). Caprock integrity of the carboniferous Frederick Brook shale analyzed by oil and gas well logs: McCully gas field and Elgin area, New Brunswick. *Geological Survey of Canada, 8203.* (120pp).

Schoell, M. (1983). Genetic characterization of natural gases. *AAPG bulletin*, *67*(12), 2225-2238.

Smith, W. D., & Gibling, M. R. (1987). Oil shale composition related to depositional setting: a case study from the Albert Formation, New Brunswick, Canada. *Bulletin of Canadian Petroleum Geology*, *35*(4), 469-487.

Smith, W. D., Peter, C. S., Naylor, R. D., Mukhopadhyay, P. K., Kalkreuth, W. D., Ball, F. D., & Macauley, G. (1991). Composition and depositional environment of major eastern Canadian oil shales. *International journal of coal geology*, *19*(1-4), 385-438.

St Peter, C. (1982, October). Geology of the Albert Formation, New Brunswick, Canada. In *Eastern Oil Shale Symposium. Kentucky Department of Energy, University of Kentucky Institute for Mining and Minerals Research, Lexington, Kentucky*.

Stueber, A. M., Walter, L. M., Huston, T. J., & Pushkar, P. (1993). Formation waters from Mississippian-Pennsylvanian reservoirs, Illinois basin, USA: Chemical and isotopic constraints on evolution and migration. *Geochimica et Cosmochimica Acta*, *57*(4), 763-784.

Tilley, B., McLellan, S., Hiebert, S., Quartero, B., Veilleux, B., & Muehlenbachs, K. (2011). Gas isotope reversals in fractured gas reservoirs of the western Canadian Foothills: Mature shale gases in disguise. *AAPG bulletin*, *95*(8), 1399-1422.

Tilley, B., & Muehlenbachs, K. (2013). Isotope reversals and universal stages and trends of gas maturation in sealed, self-contained petroleum systems. *Chemical Geology*, *339*, 194-204.

Tissot, B. P. (81). Welte. DH (1984)." Petroleum Formation and Occurrence.".

White, D. E., Hem, J. D., & Waring, G. S. (1963). *Chemical composition of subsurface waters* (No. 440-F).

Wilson, T. P., & Long, D. T. (1993). Geochemistry and isotope chemistry of Michigan Basin brines: Devonian formations. *Applied Geochemistry*, *8*(1), 81-100.

Wilson, P., White, J. C., & Roulston, B. V. (2006). Structural geology of the Penobsquis salt structure: late Bashkirian inversion tectonics in the Moncton Basin, New Brunswick, eastern Canada. *Canadian Journal of Earth Sciences*, *43*(4), 405-419.

Zeng, H., Li, J., & Liu, W. (2011, May). New insight into carbon isotopic reversals of deep gas in Songliao Basin, NE China. In *AAPG Hedberg Research Conference—Natural Gas Geochemistry: Recent Developments, Applications and Technologies*.

Zhang, M., Tang, Q., Cao, C., Lv, Z., Zhang, T., Zhang, D., ... & Du, L. (2017). Molecular and carbon isotopic variation in 3.5 years shale gas production from Longmaxi Formation in Sichuan Basin, China. *Marine and Petroleum Geology*.

Zumberge, J., Ferworn, K., & Brown, S. (2012). Isotopic reversal ('rollover') in shale gases produced from the Mississippian Barnett and Fayetteville formations. *Marine and Petroleum Geology*, *31*(1), 43-52.

Chapter 3 - Characterization of Porewater from Shallow Drill-Core Collected in Southern New Brunswick

3.1 Introduction

The characterization of pore fluids in low-permeability sedimentary formations has presented a challenge for geoscientists studying the deep geologic environments which are currently being investigated as potential targets for the sequestration of nuclear waste and carbon dioxide (Sacchi et al. 2001; Clark et al. 2013). Due to the low permeabilities of the formations under consideration, pore fluids can not be sampled effectively by conventional methods such as the use of hydraulic tests. To overcome this challenge, several methods have been developed to extract pore fluids from core samples collected from targeted formations. These methods rely on the low permeability of the rock to prevent contamination during drilling and to contain porewater after core retrieval. Once core samples are collected, porewater chemical and isotopic properties are measured in water which is extracted by squeezing, ultracentrifugation, vacuum distillation, crush-and-leach, advective displacement, and absorption into cellulose paper (Savoye et al. 2007; Altinier et al. 2007; Appelo et al. 2008; Cyr and Daidié, 2001; Clark et al. 2013; Fernández et al. 2013; Celejewski et al. 2014; Mazurek et al. 2015).

The objective of this study is to apply the cellulose-paper absorption method for porewater extraction and characterization to low-permeability rocks recovered from shallow (50-80 m) open-borehole observation wells in the McCully gas field and Elgin areas of southern New Brunswick. The implementation of these discrete profiles is intended to characterize geochemical

conditions at multiple depths, in order to better understand the role of lithology and fractures on the presence of solutes and hydrocarbons.

3.2 Study Area and Fieldwork

The McCully gas field is located in the Penobsquis area of southern New Brunswick near the town of Sussex. It produces natural gas and small amounts of condensates from 32 vertical and inclined hydraulically fractured wells in tight sandstone and shale reservoirs. The Geological Survey of Canada (GSC) is currently studying the groundwater resources of the area and assessing aquifer vulnerability to the effects of hydraulic fracturing and natural gas production. As part of this study, ten monitoring wells were constructed on well pads in the McCully field and outside the nearby town of Elgin where a few hydrocarbon exploration wells have been drilled (Fig 3.1). Six of the wells were drilled using hammer-rotary methods, and four were completed in continuously cored, diamond-drilled boreholes. A total of 61 core samples were collected for porewater extraction using the cellulose paper absorption method in order to develop detailed, depth-discrete profiles of porewater geochemistry in the area (Table 3.1). Shallow bedrock in the area is composed mostly of low-permeability mudstones, sandstone, and conglomerates, with secondary porosity in the form of fractures which act as conduits for groundwater flow. Groundwater monitoring carried out in these monitoring wells as part of the larger GSC project found little to no hydrocarbons present. Only well PO-07 showed small concentrations of methane, while PO-09 showed the presence of some ethane. Gas extracted from core samples collected in IsoJars® showed that only one sample contained low concentrations of methane (PO-09 at a depth of 60 m).

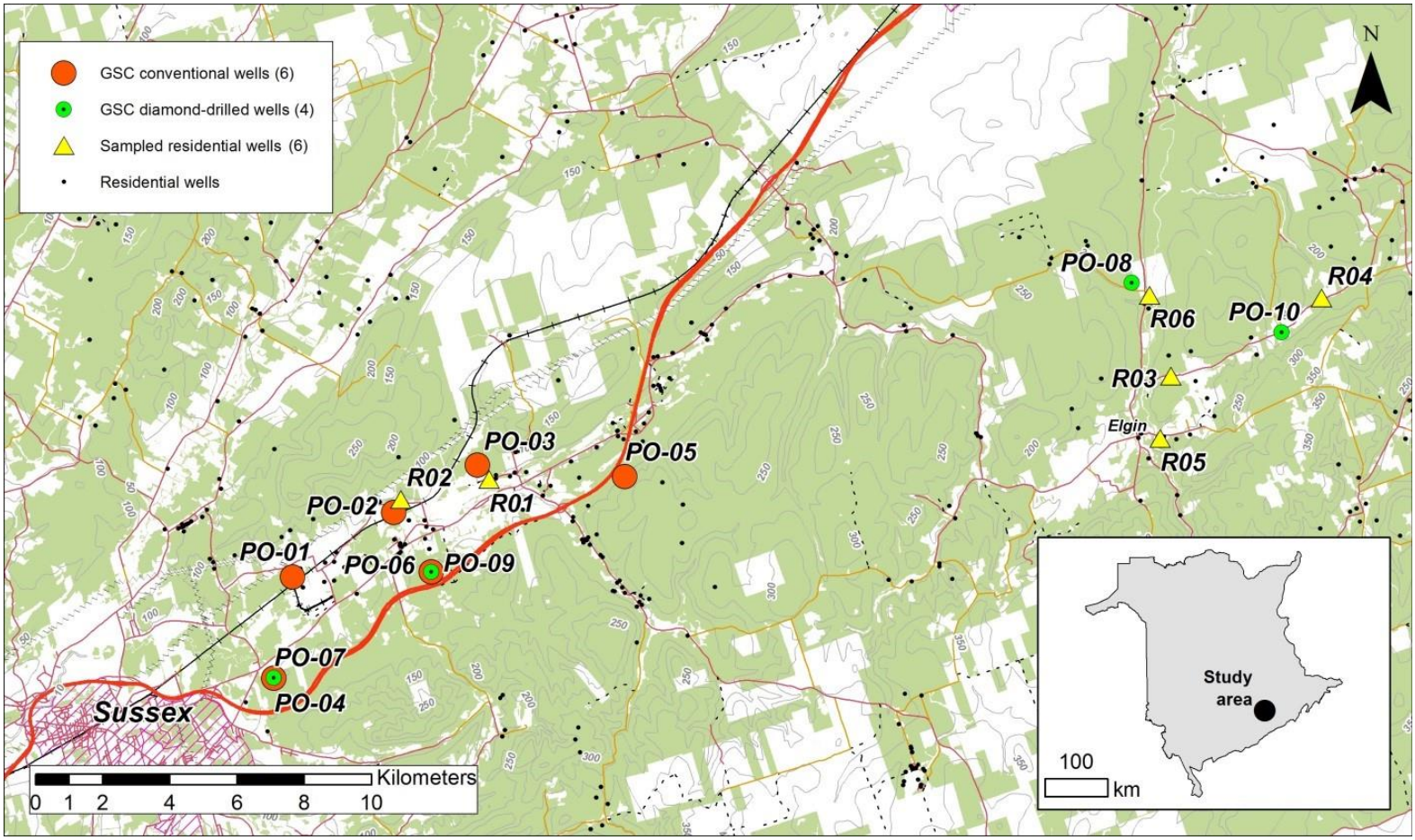

Figure 3.1. Map of GSC observation wells in the McCully and Elgin areas of New Brunswick. Core was collected from the four GSC diamond-drilled wells: PO-07, PO-08, PO-09, and PO-10.

Table 3.1. Summary of McCully – Elgin porewater extractions

Well	Area	Core samples	Porewater samples
PO-07	McCully	22	34
PO-08	Elgin	16	29
PO-09	McCully	13	27
PO-10	Elgin	10	15

Shallow bedrock in the McCully and Elgin areas belongs to the Carboniferous Mabou Group, a regressive terrestrial sequence which conformably overlies the marine rocks and evaporite deposits of the Windsor Group (Wilson and White, 2006; Huchet et al. 2017). A description of the lithologies intersected in each borehole is provided below.

PO-07

Monitoring well PO-07 was drilled to a depth of 50 m on a gas well pad in the McCully field. Lithology of consists of roughly 19 m of red mudstone overlying approximately 20 m of red gravel breccia interbedded with red mudstone. These rocks overly approximately 10 m of red siltstone and a three-meter-thick layer of heavily fractured sandstone (Fig. 3.2).

PO-08

PO-08 was drilled to a depth of approximately 40 m on a gas well pad in the Elgin area. Lithologies consist almost entirely of fine-medium sandstone with cm-thick layers of greenish-grey claystone. The most significant feature of the sandstone in PO-08 is the colour zonation, which transitions sharply back and forth between grey and reddish brown, indicating abrupt changes in redox conditions (Fig. 3.3). The reddish-brown sections are associated with increased fracturing, indicating that inflow of oxygenated meteoric water may be the cause of oxidation.

PO-09

PO-09 was drilled to a depth of approximately 80 m on a gas well pad in the McCully field. Bedrock is overlain by approximately 13.5 m of unconsolidated sediments consisting mostly of muddy glacial till. Lithologies consist mostly of green-grey-red pebble breccia with interbedded mudstone and fine-medium sandstone, all of which is fractured (Fig. 3.4).

PO-10

PO-10 was drilled in the Elgin area to a depth of approximately 50 m on a gas well pad. Lithologies consist of approximately 8 m of black shale overlying 30 m of dark grey-black mudstone and a grey-black fine sandstone (Fig. 3.5).

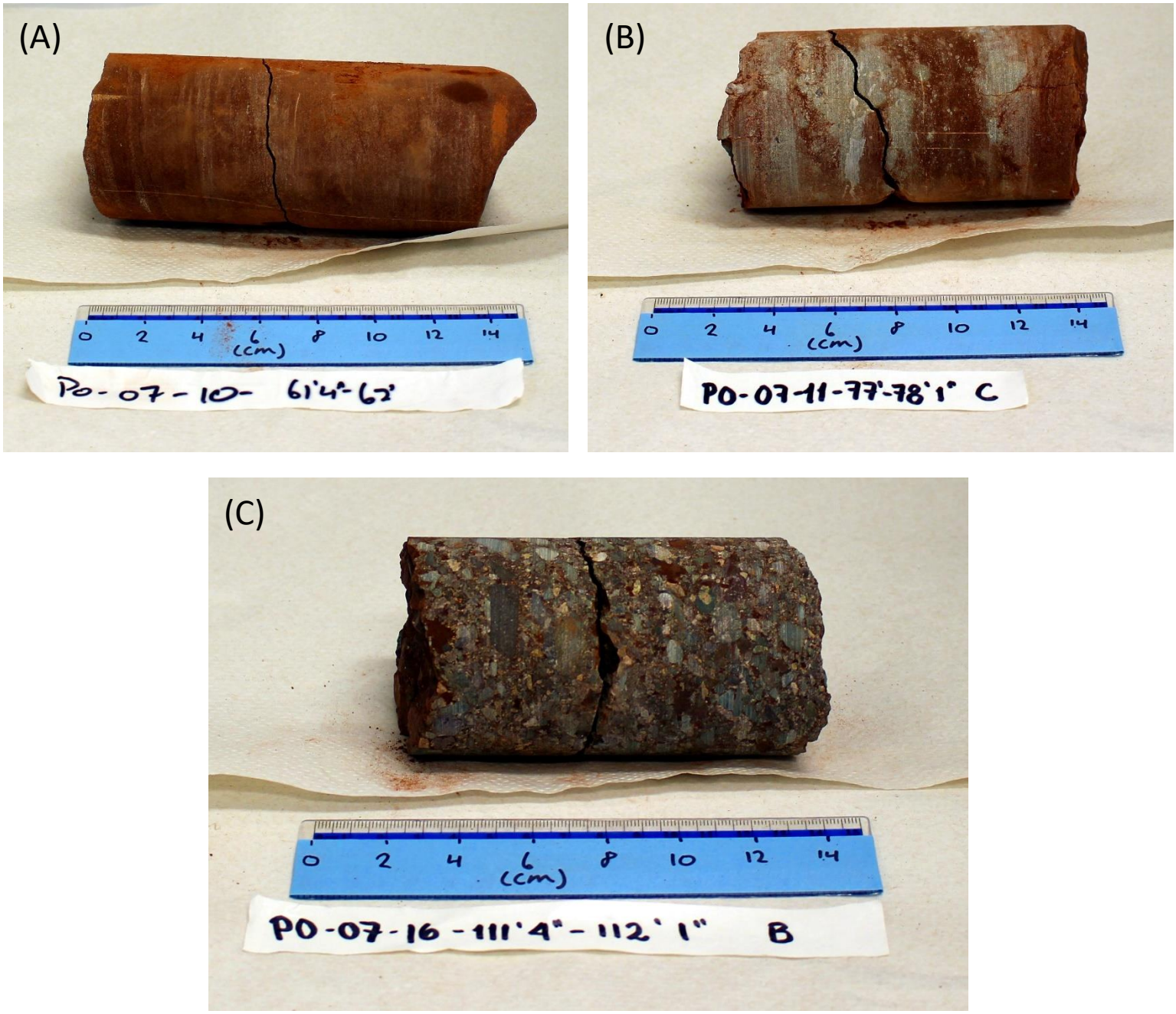

Figure 3.2. Selected core samples from PO-07. A: Red mudstone, B: Red mudstone with white mottling, C: Pebble breccia.

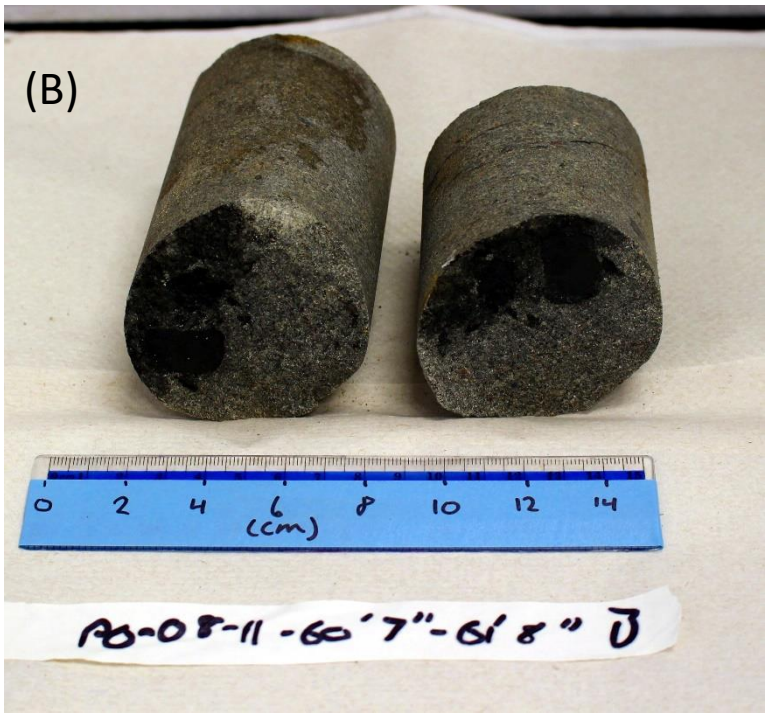

Figure 3.3. Selected core samples from PO-08. A: Grey sandstone, B: Grey sandstone showing bituminous cement C: Sandstone showing transition between red-brown, oxidized zone and grey, reduced zone.

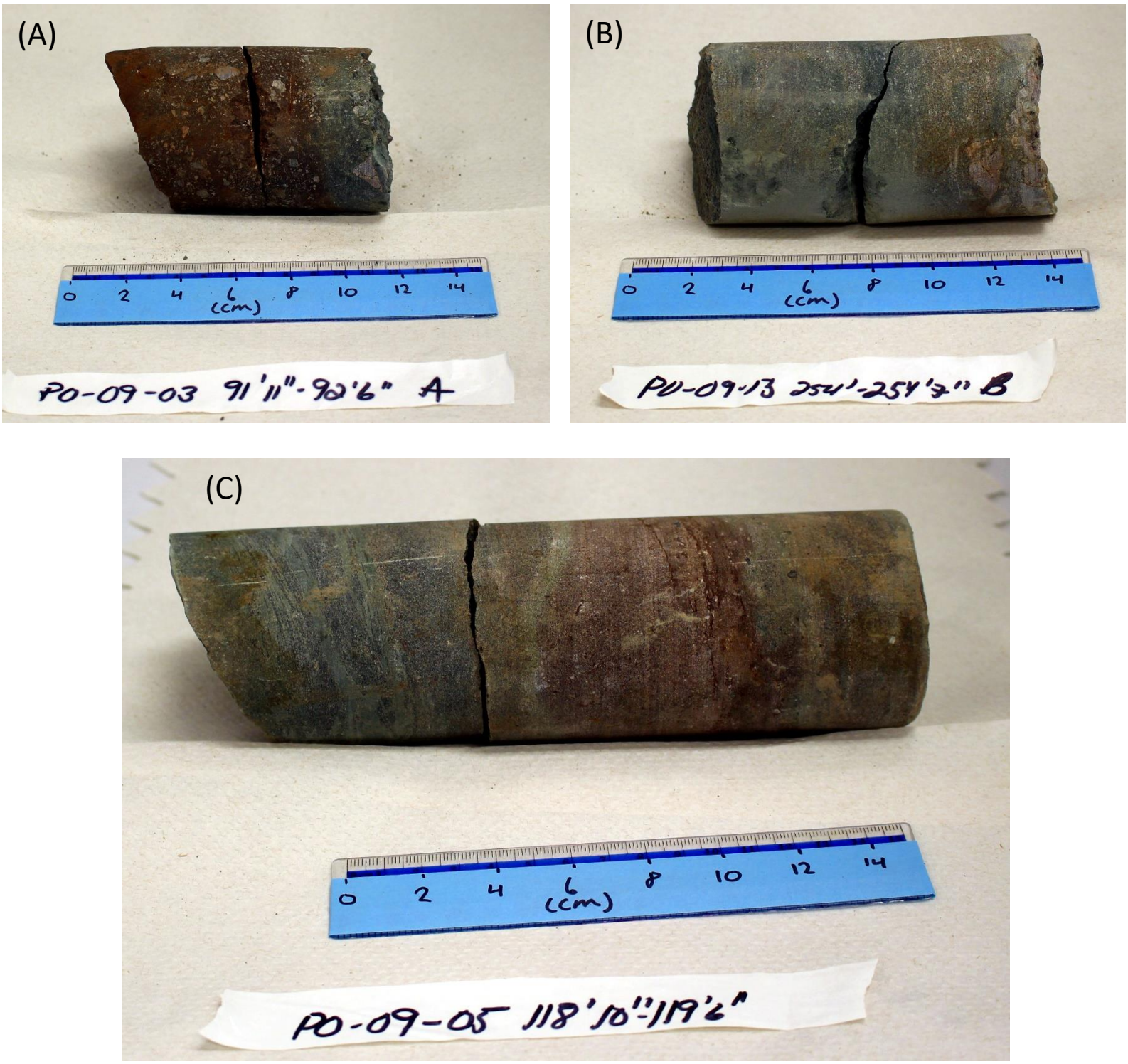

Figure 3.4. Selected core samples from PO-09. A: Red-grey pebble breccia, B: Green-grey mudstone with sand, gravel, and pebbles, C: Multicolored medium sandstone with interbedded clay.

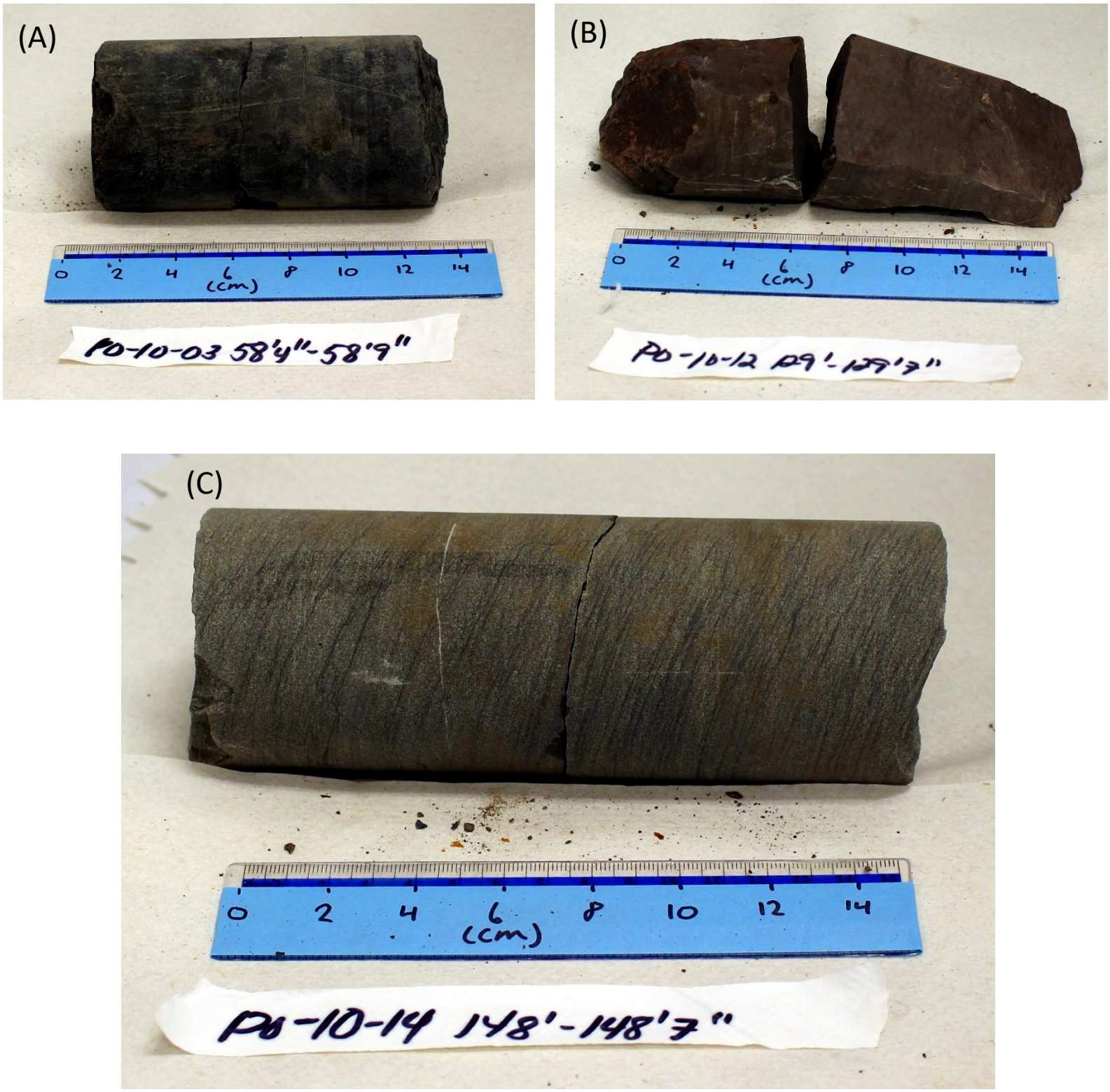

Figure 3.5. Selected core samples from PO-10. A: Dark grey-black mudstone, B: Red-brown mudstone, C: Dark grey sandstone.

3.3 Materials and Methods

3.3.1 Cellulose paper preparation

Cellulose papers (Whatman® "1 chr" cellulose chromatography paper) were cut into circles 4.5 cm in diameter. The initial water content and mass of each paper disk was measured using reflectance and transmittance Near Infrared (NIR) spectrometers and the initial "dry" mass was measured using an analytical balance. Each paper was then "sandwiched" between two disks cut from Kimwipes® laboratory wipes, 5 cm in diameter, in order to prevent transfer of rock dust to the cellulose papers during the absorption period. They were then placed inside of a sleeve made from FEP film (a transparent, thermoplastic film made of fluorinated ethylene propylene) to prevent water-vapour transfers to or from the paper, and stored in individual zip-top plastic bags.

3.3.2 Sampling

Core samples approximately 15 - 30 cm in length were collected at roughly 3 m intervals during drilling, with increased sampling around geologically interesting features such as lithology changes and fractures. Samples were stored in double vacuum-sealed bags within approximately ten minutes of being removed from the core barrel. The bags were flushed three times with nitrogen gas before being sealed in order to minimize the potential for oxidation of the samples. After sampling, cores were stored in coolers at ambient temperature and transported to the University of Ottawa.

3.3.3 Core sample preparation (core cleaving and paper insertion)

Core cleaving was performed in a humidity-controlled sample preparation room in order to minimize evaporation from fresh core faces. The cores were removed from their vacuum packing and cleaved perpendicular to the core axis using a hammer and chisel. Longer core samples were divided into multiple sub-samples to allow for replicate measurements. Immediately after the samples were split, dust and debris was removed from the fresh core-faces using a sticky tack cloth. One of the cellulose paper- Kimwipes® combinations was then placed onto a fresh core face, and the two core halves were re-united. The cores were then wrapped in plastic wrap, bound tightly with vinyl tape, sealed in vacuum packing, and stored in coolers at ambient temperature for an "absorption period" of 52 days to allow for porewater to absorb into the papers.

3.3.4 Leaching

After the absorption period, working within a humidity-controlled chamber, the cores were removed from their vacuum packing and the cellulose paper disks were removed and returned to their original FEP sleeves, the Kimwipes® disks were discarded at this time. The final water content and "wet" mass of each paper was then measured using the reflection and transmittance NIR spectrometers, and an analytical balance respectively. The papers were then placed into new 50 mL plastic centrifuge tubes to which approximately 35 mL of deionized (reverse osmosis, RO) water was added. The papers were left submerged in the RO water for a leaching period of 24 hours, after which, the leachate solutions were decanted into new 50 mL centrifuge tubes.

3.3.5 Extracted water mass measurement

Transmittance and reflection NIR-spectrometry measurements conducted before and after the papers were inserted into the cores, were used to determine the mass of porewater absorbed by the papers. The spectrometers were calibrated by adding synthetic porewater solution at various concentrations to samples of the paper and collecting spectroscopic and gravimetric data periodically as the water evaporated to dryness. The calibration process is described in detail in Celejewski et al. 2014.

3.3.6 Evaporation

After the leaching phase was complete, it was determined that concentrations of Cl, Br, and Na in the leachate solutions were too low for measurement by ICP-MS. In order to increase solute concentrations in the leachates, the solutions were placed into new 50 mL borosilicate glass beakers in five batches of 24 plus one blank, and placed on a hotplate inside of an evaporation apparatus in a "clean room" laboratory. The leachate solutions were evaporated for a period of roughly ten hours until their volumes were reduced from approximately 35 mL to 0.5 mL. The evaporated leachate solutions were then diluted to approximately 2 mL with 2% nitric acid solution and then transferred to new 15 mL plastic centrifuge tubes. The masses of the leachate solutions were measured before and after evaporation and after dilution in order to calculate concentration and dilution factors.

3.3.7 Analytical methods and quality control

Concentrations of Na, Mg, Ca, K, Fe, Sr, Cl, and Br in the evaporated leachate samples were measured by ICP-MS in the University of Ottawa geochemistry laboratory. Samples of

seawater reference (High Purity Standards #CRM-SW) as well as low and high groundwater reference standards (EnviroMAT ES-L-1, ES-H-1) were prepared and diluted to concentrations similar to those expected in the leachate solutions

Additional triplicate sets of the reference materials were prepared to assess any impacts that the evaporation process might have on measurements. 2 mL of each of the reference materials were diluted in 40 mL of RO water, the samples were then evaporated (two were evaporated to 0.5 mL and one to full dryness), then diluted to 2 mL with dilute nitric acid, using the same method as was used for the porewater samples.

3.3.8 Blanks

Paper blanks

Three paper disks, were prepared in the same way as those used to extract porewater from the cores, but were left in their plastic bags for the duration of the absorption period. They were then leached, and the solutions were evaporated, and analyzed in the same manner as the samples.

Leachate blanks

Three new 50 mL centrifuge tubes were filled with DI water in the same manner as the leachate samples. These blank solutions were then evaporated and processed in the same manner as the leachate samples.

Evaporation blanks

During each batch of evaporations, one specific beaker was filled with approximately 40 mL of MilliQ DI water and evaporated in the same manner as the leachate samples. The

evaporation blanks were diluted to 2 mL with dilute nitric acid, and processed in the same manner as all other samples.

Instrument blanks

Seven solution blanks of 2% nitric acid solution prepared with RO water were run at the beginning of the ICP-MS run.

3.4 Results and discussion

3.4.1 Quality control

Analysis of the blanks revealed contamination issues with regards to certain elements at several stages in the method (Table 3.2). The evaporation blanks were found to contain significant concentrations of sodium as well as detectable concentrations of most other solutes. Concentrations of sodium, potassium, calcium, and strontium decrease in successive evaporation blanks, indicating that leaching from the glass beakers is the most probable source. Contamination from the beakers during evaporation likely contributes a positive bias to the solute concentrations of the porewater samples which decreases in magnitude with each successive evaporation batch. The paper blank samples were found to have concentrations of sodium and chloride in excess of what was measured in all porewater samples with respect to chloride, and all but one sample with respect to sodium. Concentrations of all other analytes except for Fe, which was not detected, were present in the paper blanks at levels well below concentrations measured in the porewater samples. Concentrations in the three paper blank samples are consistent with each other and are similar to values of paper blanks in previous experiments. Solutes concentrations in the paper blank samples are believed to represents small,

intrinsic salt contents of the Whatman® "1 chr" chromatography paper, which, in addition to leaching from the beakers, likely contributes a systematic positive bias to porewater concentrations. Solute concentrations in the leachate blanks are lower than the paper blanks, yet greater than the evaporation blank for the evaporation batch in which they were evaporated (evaporation batch #5). Solutes in the leachate blanks are believed to represent a combination of leaching from the beakers and possible carry-over from previous samples. The carry-over effect is likely the result of inadequate cleaning procedures between evaporation batches, and would not be observed in the evaporation blanks, as they were all evaporated in the same beaker. Contamination from carry-over also likely contributes a positive bias to porewater solute concentrations. No solutes were measured at concentrations above the limit of detection in the instrument blanks, indicating that the RO water and plastic sample tubes used throughout the experiment do not contribute a bias to solute concentrations of the porewater samples. Iron was not present at detectable levels in any of the blanks indicating that iron concentrations of the porewater samples are not subject to contamination bias. Bromide was present at detectable levels in the paper blanks but was not present above the limit of analytical detection in any of the porewater samples.

Table 3.2. Solute concentrations of blank samples in comparison with porewater leachate samples

Blanks	Evaporation batch	Na (mg/kgw)	K (mg/kgw)	Ca (mg/kgw)	Mg (mg/kgw)	Sr (mg/kgw)	Mn (mg/kgw)	Fe (mg/kgw)	Cl (mg/kgw)	Br (mg/kgw)
Evaporation blank 1	1	0.434	0.0068	0.0032	0.00013	0.000017	-	-	0.0022	-
Evaporation blank 2	2	0.131	0.0017	0.0019	0.00014	0.000008	-	-	0.0022	-
Evaporation blank 3	3	0.039	0.0006	0.0005	0.00006	0.000006	-	-	0.0027	-
Evaporation blank 4	4	0.032	0.0006	-	0.00009	0.000012	-	-	0.0032	-
Evaporation blank 5	5	0.024	0.0006	-	0.00010	0.000009	-	-	0.0027	-
Paper blank 1	5	0.606	0.0095	0.0215	0.00226	0.000114	0.000045	-	0.299	0.0092
Paper blank 2	5	0.589	0.0086	0.0164	0.00180	0.000048	0.000046	-	0.286	0.0119
Paper blank 3	5	0.615	0.0094	0.0216	0.00220	0.000061	0.000049	-	0.303	0.012
Leachate blank 1	5	0.088	0.0032	0.0199	0.00141	0.000060	0.000101	-	0.0119	-
Leachate blank 2	5	0.093	0.0062	0.0162	0.00121	0.000058	0.000043	-	0.0123	-
Leachate blank 3	5	0.066	0.0058	0.0187	0.00161	0.000065	0.000048	-	0.0123	-
Instrument blank 1	NA	-	-	-	-	-	-	-	-	-
Instrument blank 2	NA	-	-	-	-	-	-	-	-	-
Instrument blank 3	NA	-	-	-	-	-	-	-	-	-
Instrument blank 4	NA	-	-	-	-	-	-	-	-	-
Instrument blank 5	NA	-	-	-	-	-	-	-	-	-
Instrument blank 6	NA	-	-	-	-	-	-	-	-	-
Instrument blank 7	NA	-	-	-	-	-	-	-	-	-
Samples (n = 105)										
Average[a]		0.245	0.0260	0.156	0.028	0.00093	0.00133	0.0014	0.036	-
Minimum[b]		0.037	0.0083	0.011	0.001	0.00006	0.00003	0.0002	0.012	-
Maximum[c]		0.635	0.0629	0.598	0.198	0.00688	0.0207	0.0184	0.151	-

-. Measurement below limit of detection (3x standard deviation of instrument blanks).

NA. Instrument blanks were not evaporated.

a. Average concentration of porewater leachate samples

b. Minimum concentration of porewater leachate samples

c. Maximum concentration of porewater leachate samples

3.4.2. Contamination bias correction for porewater samples

Levels of contamination for K, Ca, Mg, Sr, and Mn are relatively minor compared to the respective concentrations in porewater samples, it is therefore possible to correct the data by blank subtraction. Because contamination is believed to result from leaching from the glass beakers and papers, it is likely independent of solution volume, and is considered on a solute mass basis rather than a concentration basis. To correct for contamination bias, the porewater samples were first divided into groups according to the evaporation batch in which they were processed. On the basis of evaporation batch, the average mass of K, Ca, Mg, Sr, and Mn measured in the paper blanks was added to the masses measured in the evaporation blank, and the sum was subtracted from solute masses in the porewater sample.

$$\mathbf{M_{porewater} - (M_{PaperBlankAverage} + M_{EvaporationBlank})}$$

The concentrations of Na and Cl are higher in the blanks than what was measured in the porewater samples themselves, meaning it is impossible to correct for contamination biases, and these results cannot be used. Based on the maximum and minimum concentrations of Na and Cl in the blanks and the maximum and minimum extracted porewater masses of the papers, the detection limits for Na and Cl in the samples were determined to be 0.17 – 146.20 mg/kgw and 0.016 – 71.99 mg/kgw for respectively.

3.4.3 Absorbed water masses

Porewater masses absorbed by the papers from the cores were measured using the transmittance NIR spectra. Porewater masses for the 105 samples varied from 0.0014g in a mudstone from PO-10, to 0.046 g in a coarse sandstone from PO-09. Solute masses determined

from the leachates were normalized to the absorbed porewater mass for each sample in order to calculate in-situ porewater concentrations (Table 3.3; Figs. 3.6, 3.7, 3.8, 3.9).

Table 3.3. Results of porewater extraction and characterization

Well	Core ID	Rock type	Porewater mass extracted[a] (mg)	Average depth[b] (mbgs)	K (mg/kgw)	Ca (mg/kgw)	Mg (mg/kgw)	Sr (mg/kgw)	Mn (mg/kgw)	Fe (mg/kgw)
PO-07	01	Red mudstone	23.93	5.5	1.1	289.3	10.4	0.54	0.24	3.13
PO-07	04 A	Red mudstone	4.96	7.9	58.6	544.5	22.0	1.27	-	-
PO-07	04 B	Red mudstone	4.96	7.9	9.0	614.6	19.5	0.67	-	-
PO-07	04 C	Red mudstone	4.28	7.9	35.7	1106.9	38.0	2.60	1.91	15.81
PO-07	05	Red mudstone	7.48	8.2	20.7	678.8	25.4	1.47	0.96	10.73
PO-07	06 A	Red mudstone	3.66	12.1	100.8	814.6	39.7	2.30	-	-
PO-07	06 B	Red mudstone	5.96	12.1	62.2	660.7	36.1	1.54	4.15	15.06
PO-07	06 C	Red mudstone	5.95	12.1	170.8	1110.8	44.6	2.93	1.34	12.57
PO-07	07	Red mudstone	4.86	13.3	77.4	983.2	45.4	3.83	-	-
PO-07	08 A	Red mudstone	5.45	15.1	104.6	491.8	32.7	2.89	-	-
PO-07	08 B	Red mudstone	5.34	15.1	54.8	659.9	48.7	3.45	-	-
PO-07	09	Red mudstone	6.12	17.2	58.4	826.2	46.1	3.09	0.79	8.51
PO-07	10	Red mudstone	5.54	18.8	77.7	720.6	54.7	3.13	0.80	13.32
PO-07	11 A	Red mudstone	6.05	23.6	95.7	690.8	57.1	3.34	-	-
PO-07	11 B	Red mudstone	2.57	23.6	138.6	1701.5	91.0	7.57	-	-
PO-07	11 C	Red-grey mudstone	4.59	23.6	104.8	1288.7	64.8	6.12	-	-
PO-07	12 A	Red mudstone	6.03	26.8	83.7	454.0	38.8	1.90	-	-
PO-07	12 B	Red mudstone	5.15	26.8	40.8	812.2	57.7	3.36	3.10	11.46
PO-07	13	Red mudstone	4.37	29.1	123.2	983.3	54.2	5.62	-	14.49
PO-07	14	Red mudstone	4.41	29.5	143.7	842.3	50.7	5.66	-	-
PO-07	15 A	Red mudstone	7.33	33.5	122.4	527.9	35.5	5.68	-	-
PO-07	15 B	Red mudstone	6.59	33.5	190.0	638.1	48.8	5.64	0.82	9.75
PO-07	16 A	Red breccia	11.11	34.0	61.5	337.7	30.2	4.19	0.84	-
PO-07	16 B	Red breccia	14.48	34.0	45.7	321.5	25.1	3.60	0.38	-
PO-07	17 A	Red mudstone	2.84	35.7	174.0	966.0	79.3	11.47	-	-
PO-07	17 B	Red mudstone	3.33	35.7	179.5	861.9	65.9	9.01	-	13.12
PO-07	18	Red mudstone	5.02	38.8	157.7	879.5	71.3	11.66	-	8.21
PO-07	19	Red mudstone	3.92	41.7	369.4	2908.8	101.8	41.93	3.96	23.22
PO-07	20 A	Red mudstone	3.74	45.5	422.7	1354.2	92.9	34.09	1.59	25.00

PO-07	20 B	Red sandy mudstone	2.01	45.5	688.1	6160.5	214.2	118.27	12.16	75.91
PO-07	21 A	Red mudstone	4.16	48.4	286.5	630.6	47.1	18.27	2.41	10.62
PO-07	21 B	Red mudstone	3.65	48.4	325.5	896.3	68.9	22.27	-	12.05
PO-07	21 C	Red mudstone	2.64	48.4	433.4	1069.8	77.4	25.37	-	-
PO-07	22	Red mudstone	5.88	49.3	282.2	589.3	36.5	15.40	-	-
PO-08	01	Red-grey med SS	16.00	0.8	14.6	-	14.6	0.05	0.32	-
PO-08	02	Red Coarse SS	45.77	1.9	6.9	0.4	1.9	0.04	-	-
PO-08	03 A	Grey medium SS	25.63	3.6	24.6	255.4	242.1	0.76	9.02	2.54
PO-08	03 B	Red-grey medium SS	20.39	3.6	20.4	3.9	14.5	0.07	0.22	-
PO-08	04 A	Red-grey medium SS	20.54	4.0	4.0	-	3.0	0.00	-	-
PO-08	04 B	Grey medium SS	27.63	4.0	14.6	146.1	134.9	0.48	7.65	1.82
PO-08	04 C	Grey medium SS	30.15	4.0	12.8	145.1	128.5	0.47	9.77	1.74
PO-08	05	Grey medium SS	23.59	4.3	17.8	149.0	119.2	0.47	12.09	-
PO-08	06 A	Red medium SS	23.17	8.6	1.9	-	4.8	0.05	-	-
PO-08	06 B	Red medium SS	23.39	8.6	3.2	1.4	6.3	0.05	0.41	1.92
PO-08	07 A	Red medium SS	26.79	11.4	2.2	-	2.9	0.03	-	-
PO-08	07 B	Red medium SS	25.11	11.4	1.3	7.3	7.1	0.06	-	-
PO-08	07 C	Red-grey medium SS	19.47	11.4	10.0	5.7	8.7	0.18	-	-
PO-08	08 A	Grey medium SS	30.29	11.6	12.4	235.2	110.0	0.99	2.58	22.05
PO-08	08 B	Grey medium SS	21.51	11.6	14.9	271.9	125.2	1.32	2.65	-
PO-08	09 A	Red medium SS	26.33	13.9	3.3	-	4.8	0.10	-	-
PO-08	09 B	Grey medium SS	23.11	13.9	36.2	596.6	298.5	2.15	17.56	10.13
PO-08	11 A	Grey medium SS	35.49	18.6	10.3	565.3	57.9	1.16	18.05	4.13
PO-08	11 B	Grey medium SS, bituminous	28.94	18.6	21.1	696.6	71.4	1.27	24.82	5.36
PO-08	12	Grey medium SS	27.96	23.3	11.7	397.3	66.2	1.04	0.98	2.32
PO-08	13 A	Grey medium SS	42.13	26.5	8.8	240.6	47.1	0.94	5.04	8.07

PO-08	13 B	Grey medium SS	39.66	26.5	13.9	241.7	44.7	0.96	1.57	2.19
PO-08	14 A	Grey medium SS	22.02	28.2	21.4	586.1	76.0	1.82	2.95	6.18
PO-08	14 B	Grey medium SS	22.67	28.2	27.2	364.2	49.0	1.76	2.09	3.78
PO-08	14 C	Grey medium SS	24.23	28.2	22.0	272.4	56.3	0.40	2.18	-
PO-08	15 A	Grey medium SS	23.20	31.3	8.7	496.9	85.2	0.95	3.37	3.52
PO-08	15 B	Grey medium SS	26.52	31.3	5.0	429.2	69.3	0.80	5.13	5.15
PO-08	16 A	Grey medium SS	23.47	35.8	15.9	384.5	68.8	0.68	2.65	14.36
PO-08	16 B	Grey medium SS	24.14	35.8	6.1	436.2	75.4	0.84	2.58	11.14
PO-09	01 A	Red-green breccia	21.23	17.9	44.5	395.7	109.7	1.92	1.69	4.44
PO-09	01 B	Red-green breccia	19.42	17.9	36.8	491.6	110.3	1.71	5.28	3.10
PO-09	02 A	Grey coarse SS	14.79	25.7	31.4	306.5	86.1	1.66	5.41	4.80
PO-09	02 B	Grey coarse SS	18.75	25.7	67.4	426.6	118.3	3.12	1.76	-
PO-09	03 A	Red-brown breccia	15.07	28.1	43.4	240.4	66.9	0.87	0.96	10.09
PO-09	03 B	Grey coarse SS	12.82	28.1	58.5	594.9	163.2	1.86	0.88	5.79
PO-09	04 A	Grey medium SS	14.63	31.9	30.1	307.3	73.6	0.64	0.35	-
PO-09	04 B	Grey medium SS	14.85	31.9	40.7	221.2	65.0	0.64	1.07	-
PO-09	04 C	Grey fine SS	13.05	31.9	29.0	394.4	86.5	0.92	1.11	7.09
PO-09	04 D	Grey fine SS	9.88	31.9	37.5	248.3	57.6	0.69	0.86	-
PO-09	05	Grey fine SS	10.11	36.3	32.1	446.1	62.6	0.66	1.74	-
PO-09	06 A	Grey medium SS	16.63	39.0	11.5	291.3	50.0	0.38	0.96	6.23
PO-09	06 B	Grey-red fine SS	18.38	39.0	11.8	178.2	27.8	0.20	1.65	-
PO-09	06 C	Grey breccia	22.22	39.0	15.3	347.9	54.7	0.32	1.27	3.19
PO-09	07	Grey-green medium SS	15.01	42.5	38.7	733.5	114.3	0.77	0.45	5.59
PO-09	08 A	Red-green medium SS	12.52	45.9	38.2	247.8	34.8	0.46	0.98	-
PO-09	08 B	Red medium SS	11.13	45.9	30.8	243.5	34.1	0.70	0.70	-

PO-09	08 C	Red medium SS	6.75	45.9	47.6	511.6	73.6	0.75	1.51	16.70
PO-09	09	Grey-green medium SS	6.80	58.2	37.1	416.9	39.0	1.01	1.04	-
PO-09	10 A	Grey-green medium SS	9.31	63.4	-	406.6	41.7	0.54	-	8.53
PO-09	10 B	Grey-green medium SS	7.64	63.4	16.5	421.9	48.6	0.67	-	-
PO-09	10 C	Grey-green medium SS	9.22	63.4	16.4	429.4	45.0	0.63	-	17.17
PO-09	11 A	Grey medium SS	12.30	65.8	34.6	317.1	29.6	0.36	0.87	8.90
PO-09	11 B	Grey medium SS	7.26	65.8	38.0	388.3	44.1	0.48	0.77	-
PO-09	12	Grey-green fine SS	4.20	68.9	20.0	873.9	73.1	1.20	3.07	-
PO-09	13 A	Grey-green fine SS	9.14	77.5	68.8	782.9	85.4	1.45	1.47	7.83
PO-09	13 B	Grey-green fine SS	13.20	77.5	59.7	345.7	41.0	0.70	0.64	6.04
PO-10	01	Dark grey mudstone	6.80	8.6	28.7	759.6	275.9	7.15	15.66	77.23
PO-10	02	Dark grey mudstone	9.29	14.7	58.9	415.9	191.7	16.00	2.62	9.08
PO-10	03	Dark grey mudstone	7.21	17.8	215.8	600.8	245.3	28.66	5.75	-
PO-10	04	Dark red mudstone	13.49	18.5	79.6	267.5	119.3	12.51	1.25	4.77
PO-10	05	Dark red mudstone	1.49	21.8	263.5	1185.0	469.5	48.36	3.29	-
PO-10	06	Dark red mudstone	6.79	24.4	72.5	754.9	122.7	18.28	6.13	-
PO-10	07	Dark red mudstone	7.98	29.2	92.0	111.3	30.2	3.89	1.06	65.60
PO-10	08	Dark grey mudstone	8.45	31.0	15.1	-	2.6	0.19	0.28	-
PO-10	10 A	Light grey mudstone	2.87	36.0	-	-	-	-	-	-
PO-10	10 B	Light grey mudstone	1.40	36.0	-	110.7	51.2	1.94	-	-
PO-10	11	Dark grey mudstone	9.53	38.5	2.5	-	-	0.04	-	-
PO-10	12	Dark red mudstone	2.79	39.4	-	119.9	19.0	1.78	-	-

PO-10	13 A	Dark red fine SS	3.86	42.2	-	-	-	0.50	-	-
PO-10	13 B	Dark red fine SS	3.09	42.2	30.2	-	-	1.79	-	-
PO-10	14	Dark grey medium SS	7.61	45.2	74.1	-	-	0.44	-	-

a: Mass of porewater extracted from core sample, calculated using transmittance NIR spectra.

b: Average depth of core sample in meters below ground surface, considered accurate to ± 3 m.

-: Measurement below limit of detection.

3.4.4 Uncertainty in porewater concentrations

The uncertainty of K, Ca, Mg, and Sr concentrations in the porewater samples was calculated using the average of the relative standard deviation (RDS %) of the results from several long cores (~30 cm) which were divided into triplicate sub-core samples (Table 3.2). It is assumed that due to their low permeabilities, solute transport in these rocks is mostly controlled by diffusion, and that porewater composition is effectively homogenous over short intervals (10's of cm) of unfractured rock. Based on this assumption, it is assumed that porewater composition in sub-samples of a 30-cm core is effectively uniform, and that differences in measured porewater composition are reflective of uncertainty of the method. This is of course not the case in instances where the rock is sufficiently reactive to create significant geochemical variability over short distances such as in the red and grey colour zones observed in PO-09. In order to minimize the effects of rock reactivity, only cores that were relatively homogenous in composition and colouration were used to calculate RSD, and the results were then averaged.

Table 3.4. Relative standard deviation of porewater concentrations of triplicate sub-core samples

Well	Core IDs	K (RSD %)	Ca (RSD %)	Mg (RSD %)	Sr (RSD %)
PO-07	04 A,B,C	72.1	40.6	37.9	65.4
PO-07	06 A,B,C	49.5	26.5	10.7	30.8
PO-07	11 A,B,C	20.0	41.4	25.0	37.8
PO-08	14 A,B,C	13.6	39.6	23.0	60.4
PO-09	08 A,B,C	21.6	45.9	47.6	24.4
PO-09	10 A,B,C	-	2.8	7.6	10.9
Average		35.4	32.8	25.3	38.3

-Relative standard deviation (RSD%) is calculated as the ratio of the standard deviation and average of triplicate measurements [(STDEV(3 samples)/AVERAGE(3 samples)]x100%

The relative standard deviation of solute concentrations in the triplicate samples is quite high, indicating that they may be affected by multiple sources of error. Uncertainty of the ICP-MS analysis for K, Ca, Mg, and Sr varies from 0.5-2% RSD, and can not account for the much larger uncertainties observed. The most likely source of error affecting porewater compositions aside from analytical uncertainty, is evaporation from the fresh core faces immediately after core cleaving, and from the wet papers when they are removed from the cores. Precautions are taken to minimize evaporation, including performing the core cleaving and wet-paper removal steps of the method in humidity-controlled environments with relative humidifies of around 90%. However, due to the extremely high dilution ratios during the leaching phase (0.0014 – 0.046 g of porewater leached in 35 g of RO water), even very small amounts of evaporation, and uncertainty in water mass measurement can have a significant effect on porewater concentrations.

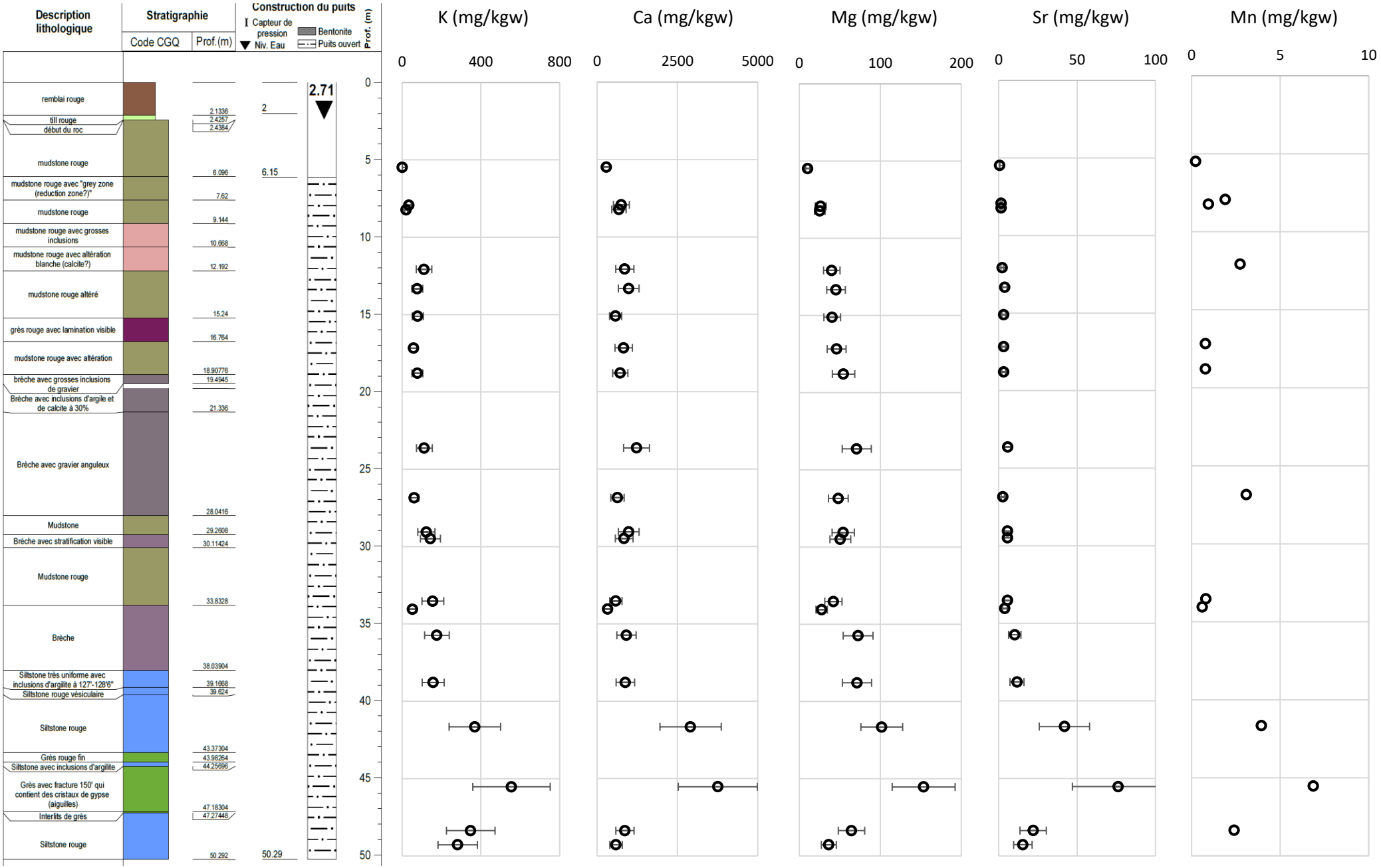

Figure 3.6. Vertical geochemical profiles of porewater from cores collected from observation well PO-07.

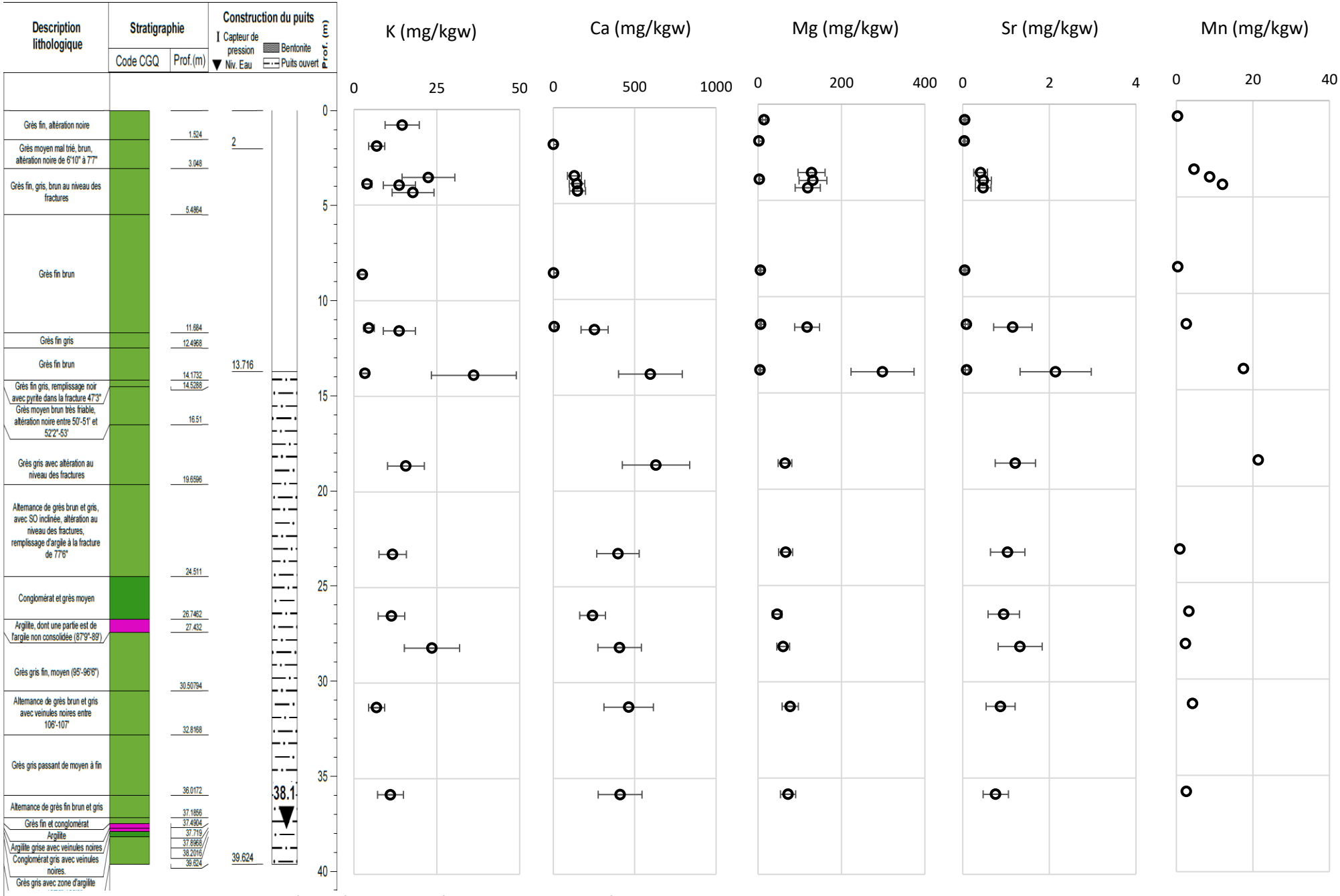

Figure 3.7. Vertical geochemical profiles of porewater from cores collected from observation well PO-08.

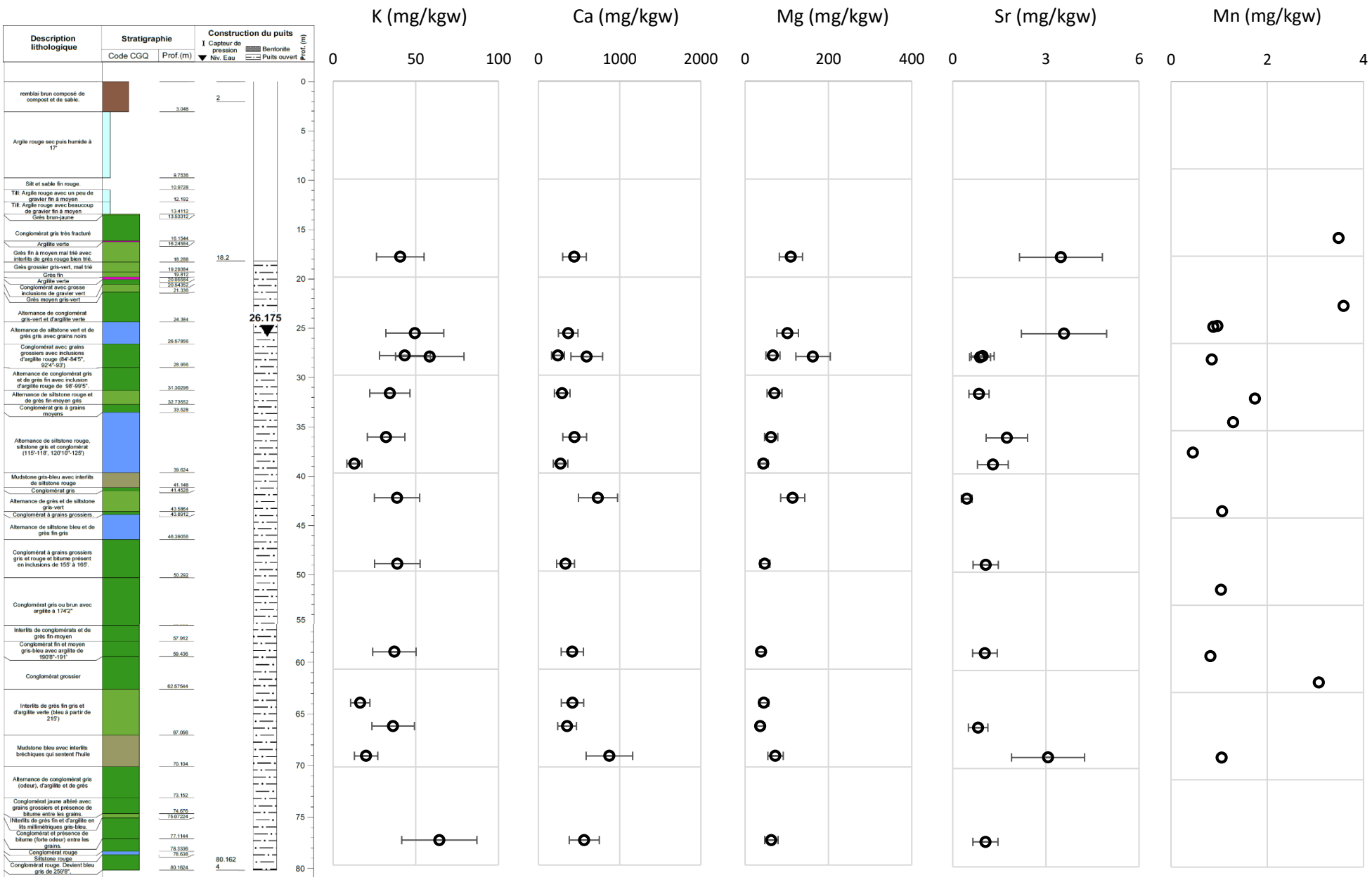

Figure 3.8. Vertical geochemical profiles of porewater from cores collected from observation well PO-09.

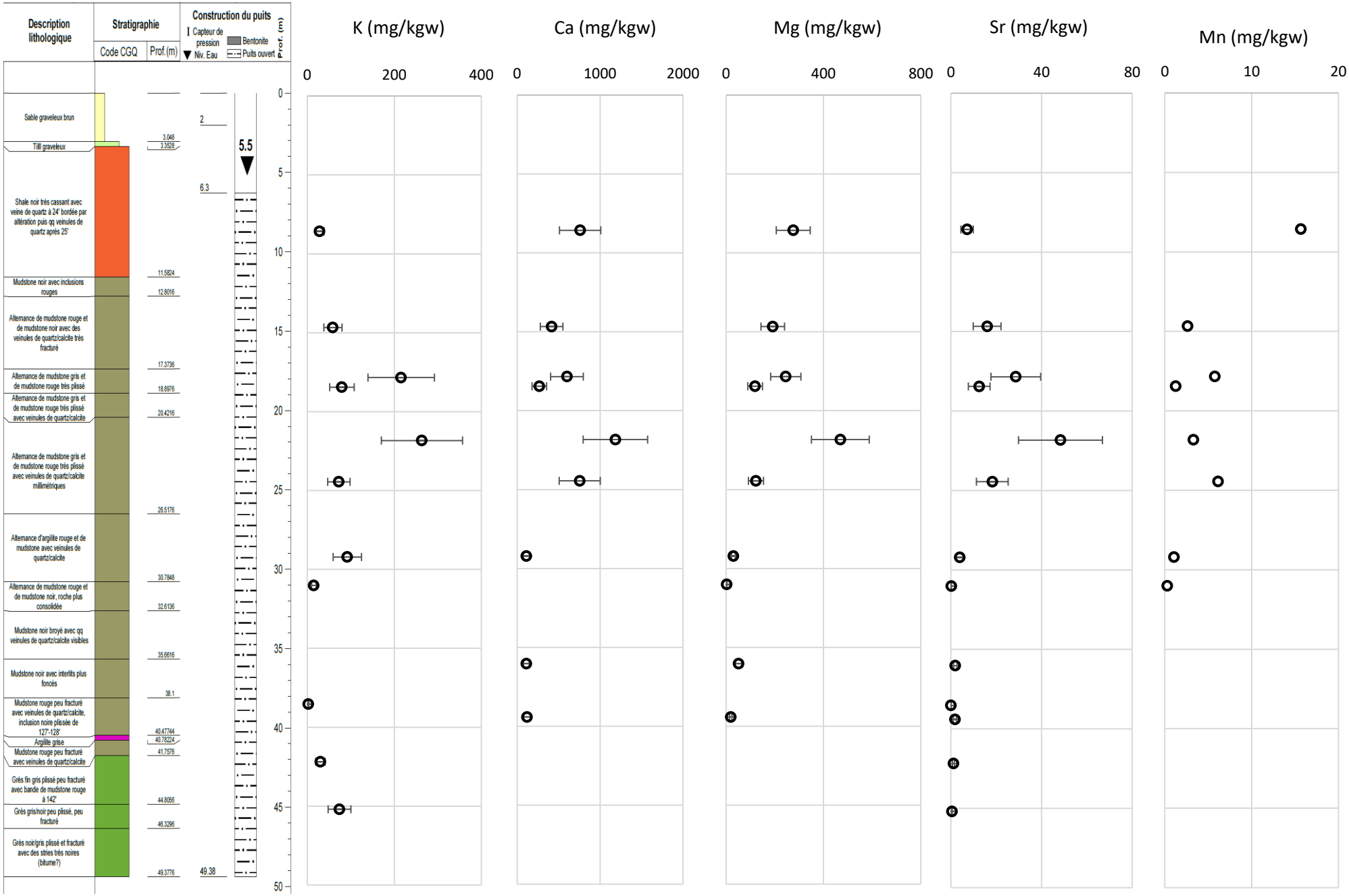

Figure 3.9. Vertical geochemical profiles of porewater from cores collected from observation well PO-10.

3.4.5 Geologic controls on porewater composition

Porewater composition in PO-07 appear to be affected by primarily rock type. Concentrations of solutes are uniform in the red mudstone and breccia samples of the first 40 m, but increase substantially in the sandstone samples between 40 and 50 m. The elevated TDS of these samples coincides with the appearance of gypsum, and may reflect an increase in rock reactivity as well as an increase in hydraulic conductivity, which may act as a conduit for higher TDS groundwater. Porewater composition in PO-08 appears to be strongly influenced by abrupt changes in rock colouration. Dramatic changes in solute concentrations are observed over very short distances between samples taken on either side of boundaries between red-brown sandstones and grey sandstones at depths of 11.5 and 13.9 m. In both cases, solute concentrations are significantly higher in the grey, reduced rocks than in the red-brown, oxidized rocks of the same type. The composition of porewater in PO-09 is relatively consistent and does not show any clear trends related to rock type. Porewater composition in PO-10 displays elevated TDS in the interval between 17 and 22 m depth. This interval does not coincide with any obvious changes in rock type or increased fracturing. Samples taken from the sandstone below 40 m depth display lower TDS, with concentrations of Ca and Mg below the limit of detection.

3.5 Conclusions

A total of 105 porewater samples were extracted from 61 shallow core samples collected from four diamond drilled monitoring wells in the McCully and Elgin areas using the paper-absorption method. The experiment was successful in characterising the K, Ca, Mg, Sr, Mn, and Fe concentrations of the porewater in most of the samples. Na, Cl, and Br were not successfully characterized in the samples due to high detection limits resulting from contamination

introduced by the paper and from glassware used for sample evaporation. Vertical geochemical profiles were prepared and plotted in relation to stratigraphic columns for the wells. These profiles reveal several insights into the hydro-geochemical controls on groundwater composition in the shallow fractured bedrock in the McCully and Elgin areas. Porewater composition in the relatively homogenous, claystone dominated bedrock of PO-07 appears to be controlled primarily by rock permeability, while porewater composition in the sandstone bedrock of PO-08 appears to be influenced heavily by changes in redox conditions, which are associated with fractures.

3.6 Recommendations for future work

Results of this experiment clearly demonstrate many of the strengths and weaknesses of the paper-absorption method for extraction characterization of porewater chemistry from low-permeability rock. One of the main advantages of the paper-absorption method is its scalability and high throughput. In this experiment, a total of six work days over a 58-day experiment period were required to produce 105 aqueous leachate samples from 61 rock samples. However, due to the relative simplicity of sample preparation and processing, doubling or tripling the number of samples would have required only a handful of additional work days over the same experiment period. In this experiment, rock samples were collected at a frequency of roughly one sample per 5 m of depth, however, this method could support substantially higher frequencies of sampling in cases where it is required in order to examine complex and intricate hydro-geochemical systems.

The greatest challenge of the paper-absorption method is the high degree of care and management required to process the extremely small volume of porewater which is extracted from the rock samples. In this experiment, porewater masses varied from 0.0014 to 0.046 g, which were diluted in 35 g of water for leaching, resulting in dilution factors of 760 to 25,000 times. Dilution factors of this magnitude, magnify the uncertainty in porewater mass measurement and require that extreme care be taken to ensure that these measurements are as accurate, consistent and un-biased as possible. The following steps should be taken to avoid uncertainty and bias related to porewater mass measurement:

a. Paper-insertion into, and removal from the core samples should be performed in an environment where humidity is controlled, and is as elevated as possible, in order to prevent evaporation of porewater from the fresh core faces after cleaving, and from the papers during removal.
b. Water mass in both the wet and dry papers should be measured as carefully as possible using the transmittance and reflectance spectrometers as well as the analytical balance, in order to provide a basis for comparison and a backup in the event of anomalous measurements. Calibration of the spectrometers should be checked before analysis of the wet and dry papers, and reference materials should be run after every ten samples to account for any instrumental drift that may occur.
c. Dilution factors of the leachates should be minimized by adding only the minimum amount of water necessary to cover the papers.

d. In the event that solute concentrations are below the limit of detection in leachate samples, evaporation is not recommended, as the increases in concentration are outweighed by excessive contamination bias.

3.7 References cited

Altinier, M. V., Savoye, S., Michelot, J. L., Beaucaire, C., Massault, M., Tessier, D., & Waber, H. N. (2007). The isotopic composition of pore-water from Tournemire argillite (France): An inter-comparison study. *Physics and Chemistry of the Earth, Parts A/B/C*, *32*(1), 209-218.

Appelo, C. A. J., Vinsot, A., Mettler, S., & Wechner, S. (2008). Obtaining the porewater composition of a clay rock by modeling the in-and out-diffusion of anions and cations from an in-situ experiment. *Journal of Contaminant Hydrology*, *101*(1), 67-76.

Celejewski, M., Scott, L., & Al, T. (2014). An absorption method for extraction and characterization of porewater from low-permeability rocks using cellulosic sheets. *Applied geochemistry*, *49*, 22-30.

Clark, I. D., Al, T., Jensen, M., Kennell, L., Mazurek, M., Mohapatra, R., & Raven, K. G. (2013). Paleozoic-aged brine and authigenic helium preserved in an Ordovician shale aquiclude. *Geology*, *41*(9), 951-954.

Cyr, M., & Daidié, A. (2007). Optimization of a high-pressure pore water extraction device. *Review of scientific instruments*, *78*(2), 023906.

Fernández, A., Sánchez-Ledesma, D., Tournassat, C., Melón, A., González, A., Gaucher, E., & Vinsot, C. (2013). Applying squeezing technique to clayrocks: lessons learned from experiments at Mont Terri Rock Laboratory. *Informes Técnicos Ciemat report*, *1300*.

Huchet, F., Rivard, C., Lefebvre, R. 2017. Hydrogeological characterization above two gas fields, Moncton sub-basin, southern New Brunswick, GeoOttawa (2017), 70th Canadian Geotechnical Conference and the 12th Joint CGS/IAH-CNC Groundwater Conference, October 1-4 2017, Ottawa, Canada.

Mazurek, M., Oyama, T., Wersin, P., Alt-Epping, P., (2015). Pore-water squeezing from indurated shales. Chem. Geol. 400, 106–121. doi:10.1016/j.chemgeo.2015.02.008

Sacchi, E., Michelot, J. L., Pitsch, H., Lalieux, P., & Aranyossy, J. F. (2001). Extraction of water and solutes from argillaceous rocks for geochemical characterization: methods, processes and current understanding. *Hydrogeology Journal*, *9*(1), 17-33.

Savoye, S., Michelot, J. L., Wittebroodt, C., & Altinier, M. V. (2006). Contribution of the diffusive exchange method to the characterization of pore-water in consolidated argillaceous rocks. *Journal of contaminant hydrology*, *86*(1), 87-104.